Contents

Chapter 19

Magnetohydrodynamics

Version 1219.2.K.pdf, 14 October 2013
Please send comments, suggestions, and errata via email to kip@caltech.edu or on paper to Kip Thorne, 350-17 Caltech, Pasadena CA 91125

Box 19.1
Reader's Guide

- This chapter relies heavily on Chap. 13 and somewhat on the treatment of vorticity transport in Sec. 14.2
- Part VI, Plasma Physics (Chaps. 20-23) relies heavily on this chapter.

19.1 Overview

In preceding chapters, we have described the consequences of incorporating viscosity and thermal conductivity into the description of a fluid. We now turn to our final embellishment of fluid mechanics, in which the fluid is electrically conducting and moves in a magnetic field. The study of flows of this type is known as *Magnetohydrodynamics* or MHD for short. In our discussion, we eschew full generality and with one exception just use the basic Euler equation (no viscosity, no heat diffusion, ...) augmented by magnetic terms. This suffices to highlight peculiarly magnetic effects and is adequate for many applications.

The simplest example of an electrically conducting fluid is a liquid metal, for example mercury or liquid sodium. However, the major application of MHD is in plasma physics—Part VI. (A plasma is a hot, ionized gas containing free electrons and ions.) It is by no means obvious that plasmas can be regarded as fluids, since the mean free paths for Coulomb-force collisions between a plasma's electrons and ions are macroscopically long. However, as we shall learn in Sec. 20.5, collective interactions between large numbers of plasma particles can isotropize the particles' velocity distributions in some local mean reference frame, thereby making it sensible to describe the plasma macroscopically by a mean density, velocity, and

pressure. These mean quantities can then be shown to obey the same conservation laws of mass, momentum and energy, as we derived for fluids in Chap. 13. As a result, a fluid description of a plasma is often reasonably accurate. We defer to Part VI further discussion of this point, asking the reader to take it on trust for the moment. In MHD, we also, implicitly, assume that the average velocity of the ions is nearly the same as the average velocity of the electrons. This is usually a good approximation; if it were not so, then the plasma would carry an unreasonably large current density.

There are two serious technological applications of MHD that may become very important in the future. In the first, strong magnetic fields are used to confine rings or columns of hot plasma that (it is hoped) will be held in place long enough for thermonuclear fusion to occur and for net power to be generated. In the second, which is directed toward a similar goal, liquid metals or plasmas are driven through a magnetic field in order to generate electricity. The study of magnetohydrodynamics is also motivated by its widespread application to the description of space (within the solar system) and astrophysical plasmas (beyond the solar system). We shall illustrate the principles of MHD using examples drawn from all of these areas.

After deriving the basic equations of MHD (Sec. 19.2), we shall elucidate magnetostatic (also called hydromagnetic) equilibria by describing a *Tokamak* (Sec. 19.3). This is currently the most popular scheme for magnetic confinement of hot plasma. In our second application (Sec. 19.4) we shall describe the flow of conducting liquid metals or plasma along magnetized ducts and outline its potential as a practical means of electrical power generation and spacecraft propulsion. We shall then return to the question of magnetostatic confinement of hot plasma and focus on the stability of equilibria (Sec. 19.5). This issue of stability has occupied a central place in our development of fluid mechanics and it will not come as a surprise to learn that it has dominated research into thermonuclear fusion in plasmas. When a magnetic field plays a role in the equilibrium (e.g. for magnetic confinement of a plasma), the field also makes possible new modes of oscillation, and some of these MHD modes can be unstable to exponential growth. Many magnetic confinement geometries exhibit such instabilities. We shall demonstrate this qualitatively by considering the physical action of the magnetic field, and also formally using variational methods.

In Sec. 19.6 we shall turn to a geophysical problem, the origin of the earth's magnetic field. It is generally believed that complex fluid motions within the earth's liquid core are responsible for regenerating the field through dynamo action. We shall use a simple model to illustrate this process.

When magnetic forces are added to fluid mechanics, a new class of waves, called magnetosonic waves, can propagate. We conclude our discussion of MHD in Sec. 19.7 by deriving the properties of these wave modes in a homogeneous plasma and discussing how they control the propagation of cosmic rays in the interplanetary and interstellar media.

19.2 Basic Equations of MHD

The equations of MHD describe the motion of a conducting fluid in a magnetic field. This fluid is usually either a liquid metal or a plasma. In both cases, the conductivity, strictly speaking, should be regarded as a tensor if the electrons' cyclotron frequency (Sec. 20.6.1)

Fig. 19.1: The two key physical effects that occur in MHD. (a) A moving conductor modifies the magnetic field by appearing to drag the field lines with it. When the conductivity is infinite, the field lines appear to be frozen into the moving conductor. (b) When electric current, flowing in the conductor, crosses magnetic field lines there will be a Lorentz force, which will accelerate the fluid.

exceeds their collision frequency (one over the mean time between collisions; Sec. 20.4.1). (If there are several collisions per cyclotron orbit, then the influence of the magnetic field on the transport coefficients will be minimal.) However, in order to keep the mathematics simple, we shall treat the conductivity as a constant scalar, κ_e. In fact, it turns out that, for many of our applications, it is adequate to take the conductivity as infinite, and it matters not whether that infinity is a scalar or a tensor!

There are two key physical effects that occur in MHD, and understanding them well is the key to developing physical intuition. The first effect arises when a good conductor moves into a magnetic field (Fig. 19.1a). Electric current is induced in the conductor which, by Lenz's law, creates its own magnetic field. This induced magnetic field tends to cancel the original, externally supported field, thereby, in effect, excluding the magnetic field lines from the conductor. Conversely, when the magnetic field penetrates the conductor and the conductor is moved out of the field, the induced field reinforces the applied field. The net result is that the lines of force appear to be dragged along with the conductor – they "go with the flow". Naturally, if the conductor is a fluid with complex motions, the ensuing magnetic field distribution can become quite complex, and the current will build up until its growth is balanced by Ohmic dissipation.

The second key effect is dynamical. When currents are induced by a motion of a conducting fluid through a magnetic field, a Lorentz (or $\mathbf{j} \times \mathbf{B}$) force will act on the fluid and modify its motion (Fig. 19.1b). In MHD, the motion modifies the field and the field, in turn, reacts back and modifies the motion. This makes the theory highly non-linear.

Before deriving the governing equations of MHD, we should consider the choice of primary variables. In electromagnetic theory, we specify the spatial and temporal variation of either the electromagnetic field or its source, the electric charge density and current density. One choice is computable (at least in principle) from the other using Maxwell's equations, augmented by suitable boundary conditions. So it is with MHD and the choice depends on convenience. It turns out that for the majority of applications, it is most instructive to deal

with the magnetic field as primary, and use Maxwell's equations

$$\boxed{\boldsymbol{\nabla}\cdot\mathbf{E}=\frac{\rho_e}{\epsilon_0}\,,\quad \boldsymbol{\nabla}\cdot\mathbf{B}=0\,,\quad \boldsymbol{\nabla}\times\mathbf{E}=-\frac{\partial\mathbf{B}}{\partial t}\,,\quad \boldsymbol{\nabla}\times\mathbf{B}=\mu_0\mathbf{j}+\mu_0\epsilon_0\frac{\partial\mathbf{E}}{\partial t}} \tag{19.1}$$

to express the electric field $\mathbf{E}$, the current density $\mathbf{j}$, and the charge density ρ_e in terms of the magnetic field (next subsection).

19.2.1 Maxwell's Equations in the MHD Approximation

Ohm's law, as normally formulated, is valid only in the rest frame of the conductor. In particular, for a conducting fluid, Ohm's law relates the current density $\mathbf{j}'$ measured in the fluid's local rest frame, to the electric field $\mathbf{E}'$ measured there:

$$\mathbf{j}' = \kappa_e \mathbf{E}', \tag{19.2}$$

where κ_e is the electric conductivity. Because the fluid is generally accelerated, $d\mathbf{v}/dt \neq 0$, its local rest frame is generally not inertial. Since it would produce a terrible headache to have to transform time and again from some inertial frame to the continually changing local rest frame when applying Ohm's law, it is preferable to reformulate Ohm's law in terms of the fields $\mathbf{E}$, $\mathbf{B}$ and $\mathbf{j}$ measured in the inertial frame. To facilitate this (and for completeness), we shall explore the frame dependence of all our electromagnetic quantities $\mathbf{E}$, $\mathbf{B}$, $\mathbf{j}$ and ρ_e.

We shall assume, throughout our development of magnetohydrodynamics, that the fluid moves with a non-relativistic speed $v \ll c$ relative to our chosen reference frame. We can then express the rest-frame electric field in terms of the inertial-frame electric and magnetic fields as

$$\mathbf{E}' = \mathbf{E} + \mathbf{v}\times\mathbf{B}\,;\quad E' = |\mathbf{E}'| \ll E \quad \text{so} \quad \mathbf{E} \simeq -\mathbf{v}\times\mathbf{B}\,. \tag{19.3a}$$

In the first equation we have set the Lorentz factor $\gamma \equiv 1/\sqrt{1-v^2/c^2}$ to unity consistent with our nonrelativistic approximation. The second equation follows from the high conductivity of the fluid, which guarantees that current will quickly flow in whatever manner it must to annihilate any electric field $\mathbf{E}'$ that might be formed in the fluid's rest frame. By contrast with the extreme frame dependence (19.3a) of the electric field, the magnetic field is essentially the same in the fluid's local rest frame as in the laboratory. More specifically, the analog of Eq. (19.3a) is $\mathbf{B}' = \mathbf{B} - (\mathbf{v}/c^2)\times\mathbf{E}$; and since $E \sim vB$, the second term is of magnitude $(v/c)^2 B$, which is negligible, giving

$$\mathbf{B}' \simeq \mathbf{B}\,. \tag{19.3b}$$

Because $\mathbf{E}$ is very frame dependent, so is its divergence, the electric charge density ρ_e. In the laboratory frame, where $E \sim vB$, Gauss's and Ampére's laws [the first and fourth of Eqs. (19.1)] imply that $\rho_e \sim \epsilon_0 vB/L \sim (v/c^2)j$, where L is the lengthscale on which $\mathbf{E}$ and $\mathbf{B}$ vary; and the relation $E' \ll E$ with Gauss's law implies $|\rho_e'| \ll |\rho_e|$:

$$\rho_e \sim j\,v/c^2\,,\quad |\rho_e'| \ll |\rho_e|\,. \tag{19.3c}$$

By transforming the current density between frames and approximating $\gamma \simeq 1$, we obtain $\mathbf{j}' = \mathbf{j} + \rho_e\mathbf{v} = \mathbf{j} + O(v/c)^2 j$; so in the nonrelativistic limit (first order in v/c) we can ignore the charge density and write

$$\mathbf{j}' = \mathbf{j}\,. \tag{19.3d}$$

To recapitulate, *in nonrelativistic magnetohydrodynamic flows, the magnetic field and current density are frame independent up to fractional corrections of order* $(v/c)^2$*, while the electric field and charge density are very frame dependent and are generally small in the sense that* $E/c \sim (v/c)B \ll B$ *and* $\rho_e \sim (v/c^2)j \ll j/c$ [in Gaussian cgs units $E \sim (v/c)B \ll B$ and $\rho_e c \sim (v/c)j \ll j$].

Combining Eqs. (19.2), (19.3a) and (19.3d), we obtain the nonrelativistic form of Ohm's law in terms of quantities measured in our chosen inertial, laboratory frame:

$$\mathbf{j} = \kappa_e(\mathbf{E} + \mathbf{v} \times \mathbf{B}) \; . \tag{19.4}$$

We are now ready to derive explicit equations for the (inertial-frame) electric field and current density in terms of the (inertial-frame) magnetic field. In our derivation, we will denote by L the lengthscale on which the magnetic field changes.

We begin with Ampere's law written as $\boldsymbol{\nabla} \times \mathbf{B} - \mu_0 \mathbf{j} = \mu_0 \epsilon_0 \partial \mathbf{E}/\partial t = (1/c^2)\partial \mathbf{E}/\partial t$, and we notice that the time derivative of $\mathbf{E}$ is of order $Ev/L \sim Bv^2/L$ (since $E \sim vB$). Therefore, the right-hand side is $O(Bv^2/c^2L)$ and thus can be neglected compared to the $O(B/L)$ term on the left, yielding:

$$\boxed{\mathbf{j} = \frac{1}{\mu_0} \boldsymbol{\nabla} \times \mathbf{B}} \; . \tag{19.5a}$$

We next insert this expression for $\mathbf{j}$ into the inertial-frame Ohm's law (19.4), thereby obtaining

$$\boxed{\mathbf{E} = -\mathbf{v} \times \mathbf{B} + \frac{1}{\kappa_e \mu_0} \boldsymbol{\nabla} \times \mathbf{B}} \; . \tag{19.5b}$$

If we happen to be interested in the charge density (which is rare in MHD), we can compute it by taking the divergence of this electric field.

$$\boxed{\rho_e = -\epsilon_0 \boldsymbol{\nabla} \cdot (\mathbf{v} \times \mathbf{B})} \; . \tag{19.5c}$$

Equations (19.5) express all the secondary electromagnetic variables in terms of our primary one, $\mathbf{B}$. This has been possible because of the high electric conductivity κ_e and our choice to confine ourselves to nonrelativistic (low-velocity) situations; it would not be possible otherwise.

We next derive an evolution law for the magnetic field by taking the curl of Eq. (19.5b), using Maxwell's equation $\boldsymbol{\nabla} \times \mathbf{E} = -\partial \mathbf{B}/\partial t$ and the vector identity $\boldsymbol{\nabla} \times (\boldsymbol{\nabla} \times \mathbf{B}) = \boldsymbol{\nabla}(\boldsymbol{\nabla} \cdot \mathbf{B}) - \nabla^2 \mathbf{B}$, and using $\boldsymbol{\nabla} \cdot \mathbf{B} = 0$. The result is

$$\boxed{\frac{\partial \mathbf{B}}{\partial t} = \boldsymbol{\nabla} \times (\mathbf{v} \times \mathbf{B}) + \left(\frac{1}{\mu_0 \kappa_e}\right) \nabla^2 \mathbf{B}} \; , \tag{19.6}$$

which, using Eq. (14.5) with $\boldsymbol{\omega}$ replaced by $\mathbf{B}$, can also be written as

$$\frac{D\mathbf{B}}{Dt} = -\mathbf{B} \boldsymbol{\nabla} \cdot \mathbf{v} + \left(\frac{1}{\mu_0 \kappa_e}\right) \nabla^2 \mathbf{B} \; , \tag{19.7}$$

where D/Dt is the fluid derivative defined in Eq. (14.5). When the flow is incompressible (as it usually will be), the $\boldsymbol{\nabla}\cdot\mathbf{v}$ term vanishes.

Equation (19.6) or equivalently (19.7) is called the *induction equation* and describes the temporal evolution of the magnetic field. It is the same in form as the propagation law for vorticity $\boldsymbol{\omega}$ in a flow with $\boldsymbol{\nabla}P\times\boldsymbol{\nabla}\rho=0$ [Eq. (14.3), or (14.6) with $\boldsymbol{\omega}\boldsymbol{\nabla}\cdot\mathbf{v}$ added in the compressible case]. The $\boldsymbol{\nabla}\times(\mathbf{v}\times\mathbf{B})$ term in Eq. (19.6) dominates when the conductivity is large, and can be regarded as describing the freezing of magnetic field lines into the fluid in the same way as the $\boldsymbol{\nabla}\times(\mathbf{v}\times\boldsymbol{\omega})$ term describes the freezing of vortex lines into a fluid with small viscosity ν; cf. Fig. 19.2. By analogy with Eq. (14.10), when flux-freezing dominates, the fluid derivative of $\mathbf{B}/\rho$ can be written as

$$\frac{D}{Dt}\left(\frac{\mathbf{B}}{\rho}\right)\equiv\frac{d}{dt}\left(\frac{\mathbf{B}}{\rho}\right)-\left(\frac{\mathbf{B}}{\rho}\cdot\nabla\right)\mathbf{v}=0 \tag{19.8}$$

(where ρ is mass density, not to be confused with charge density ρ_e). This says that $\mathbf{B}/\rho$ evolves in the same manner as the separation $\Delta\mathbf{x}$ between two points in the fluid; cf. Fig. 14.4 and associated discussion.

The term $(1/\mu_0\kappa_e)\nabla^2\mathbf{B}$ in the B-field evolution equation (19.6) or (19.7) is analogous to the vorticity diffusion term $\nu\nabla^2\boldsymbol{\omega}$ in the vorticity evolution equation (14.3) or (14.6). Therefore, when κ_e is not too large, magnetic field lines will diffuse through the fluid. The effective diffusion coefficient (analogous to ν) is

$$\boxed{D_M=1/\mu_0\kappa_e}\,. \tag{19.9a}$$

The earth's magnetic field provides an example of field diffusion. That field is believed to be supported by electric currents flowing in the earth's iron core. Now, we can estimate the electric conductivity of iron under these conditions and from it deduce a value for the diffusivity, $D_M\sim 1\ \mathrm{m^2 s^{-1}}$. The size of the earth's core is $L\sim 10^4$km, so if there were no fluid motions, then we would expect the magnetic field to diffuse out of the core and escape from the earth in a time

$$\boxed{\tau_M\sim\frac{L^2}{D_M}} \tag{19.9b}$$

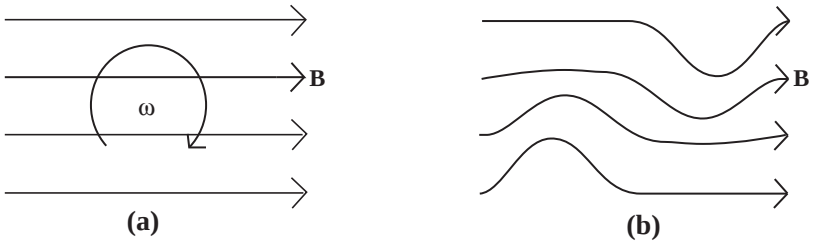

Fig. 19.2: Pictorial representation of the evolution of the magnetic field in a fluid endowed with infinite electrical conductivity. a) A uniform magnetic field at time $t=0$ in a vortex. b) At a later time, when the fluid has rotated through $\sim 30°$, the circulation has stretched and distorted the magnetic field.

$\sim$ three million years, which is much shorter than the age of the earth, ~ 5 billion years. The reason for this discrepancy, as we shall discuss in Sec. 19.6, is that there are internal circulatory motions in the liquid core that are capable of regenerating the magnetic field through dynamo action.

Although Eq. (19.6) describes a genuine diffusion of the magnetic field, to compute with confidence the resulting magnetic decay time, one must solve the complete boundary value problem. To give a simple illustration, suppose that a poor conductor (e.g. a weakly ionized column of plasma) is surrounded by an excellent conductor (e.g. the metal walls of the container in which the plasma is contained), and that magnetic field lines supported by wall currents thread the plasma. The magnetic field will only diminish after the wall currents undergo Ohmic dissipation and this can take much longer than the diffusion time for the plasma column alone.

It is customary to introduce a dimensionless number called the *Magnetic Reynolds number*, R_M, directly analogous to the fluid Reynolds number Re, to describe the relative importance of flux freezing and diffusion. The fluid Reynolds number can be regarded as the ratio of the magnitude of the vorticity-freezing term $\boldsymbol{\nabla}\times(\mathbf{v}\times\boldsymbol{\omega})\sim(V/L)\omega$ in the vorticity evolution equation $\partial\boldsymbol{\omega}/\partial t=\boldsymbol{\nabla}\times(\mathbf{v}\times\boldsymbol{\omega})+\nu\nabla^2\boldsymbol{\omega}$ to the magnitude of the diffusion term $\nu\nabla^2\boldsymbol{\omega}\sim(\nu/L^2)\omega$: $\mathrm{Re}=(V/L)(\nu/L^2)^{-1}=VL/\nu$. Here V is a characteristic speed and L a characteristic lengthscale of the flow. Similarly, the Magnetic Reynolds number is the ratio of the magnitude of the magnetic-flux-freezing term $\boldsymbol{\nabla}\times(\mathbf{v}\times\mathbf{B})\sim(V/L)B$ to the magnitude of the magnetic-flux-diffusion term $D_M\nabla^2\mathbf{B}=(1/\mu_o\kappa_e)\nabla^2\mathbf{B}\sim B/(\mu_o\kappa_e L^2)$ in the induction equation (magnetic-field evolution equation) (19.6):

$$\boxed{R_M=\frac{V/L}{D_M/L^2}=\frac{VL}{D_M}=\mu_0\kappa_e VL}\,. \tag{19.9c}$$

When $R_M\gg 1$, the field lines are effectively frozen into the fluid; when $R_M\ll 1$, Ohmic dissipation is dominant and the field lines easily diffuse through the fluid.

Magnetic Reynolds numbers and diffusion times for some typical MHD flows are given in Table 19.1. For most laboratory conditions, R_M is modest, which means that electric resistivity $1/\kappa_e$ is significant and the magnetic diffusivity D_M is rarely negligible. By contrast, in space physics and astrophysics, R_M is usually very large, $R_M\gg 1$, so the resistivity can be ignored *almost always and everywhere*. This limiting case, when the electric conductivity is treated as infinite, is often called *perfect MHD*.

Substance	L, m	V, m s^{-1}	D_M, m^2 s^{-1}	τ_M, s	R_M
Mercury	0.1	0.1	1	0.01	0.01
Liquid Sodium	0.1	0.1	0.1	0.1	0.1
Laboratory Plasma	1	100	10	0.1	10
Earth's Core	10^7	0.1	1	10^{14}	10^6
Interstellar Gas	10^{17}	10^3	10^3	10^{31}	10^{17}

Table 19.1: Characteristic Magnetic diffusivities D_M, decay times τ_M and Magnetic Reynolds Numbers R_M for some common MHD flows with characteristic length scales L and velocities V.

The phrase *almost always and everywhere* needs clarification. Just as for large-Reynolds-number fluid flows, so also here, boundary layers and discontinuities can be formed, in which the gradients of physical quantities are automatically large enough to make $R_M \sim 1$ locally. An important example discussed in Sec. 19.6.3 is *magnetic reconnection*. This occurs when regions magnetized along different directions are juxtaposed, for example when the solar wind encounters the earth's magnetosphere. In such discontinuities and boundary layers, magnetic diffusion and Ohmic dissipation are important; and, as in ordinary fluid mechanics, these dissipative layers and discontinuities can control the character of the overall flow despite occupying a negligible fraction of the total volume.

19.2.2 Momentum and Energy Conservation

The fluid dynamical aspects of MHD are handled by adding an electromagnetic force term to the Euler or Navier-Stokes equation. The magnetic force density $\mathbf{j} \times \mathbf{B}$ is the sum of the Lorentz forces acting on all the fluid's charged particles in a unit volume. There is also an electric force density $\rho_e \mathbf{E}$, but this is smaller than $\mathbf{j} \times \mathbf{B}$ by a factor $O(v^2/c^2)$ by virtue of Eqs. (19.5), so we shall ignore it. When $\mathbf{j} \times \mathbf{B}$ is added to the Euler equation (13.44) [or equivalently to the Navier-Stokes equation with the viscosity neglected as unimportant in the situations we shall study], it takes the following form:

$$\boxed{\rho \frac{d\mathbf{v}}{dt} = \rho \mathbf{g} - \boldsymbol{\nabla} P + \mathbf{j} \times \mathbf{B} = \rho \mathbf{g} - \boldsymbol{\nabla} P + \frac{(\boldsymbol{\nabla} \times \mathbf{B}) \times \mathbf{B}}{\mu_0}} \, . \tag{19.10}$$

Here we have used expression (19.5a) for the current density in terms of the magnetic field. This is our basic MHD force equation.

Like all other force densities in this equation, the magnetic one $\mathbf{j} \times \mathbf{B}$ can be expressed as minus the divergence of a stress tensor, the magnetic portion of the Maxwell stress tensor,

$$\boxed{\mathbf{T}_M = \frac{B^2 \mathbf{g}}{2\mu_0} - \frac{\mathbf{B} \otimes \mathbf{B}}{\mu_0}} \, ; \tag{19.11}$$

see Ex. 19.1. By virtue of $\mathbf{j} \times \mathbf{B} = -\boldsymbol{\nabla} \cdot \mathbf{T}_M$ and other relations explored in Sec. 13.5 and Box 13.4, we can convert the force-balance equation (19.10) into the conservation law for momentum [generalization of Eq. (13.42)]

$$\frac{\partial (\rho \mathbf{v})}{\partial t} + \nabla \cdot (P \mathbf{g} + \rho \mathbf{v} \otimes \mathbf{v} + \mathbf{T}_g + \mathbf{T}_M) = 0 \, . \tag{19.12}$$

Here $\mathbf{T}_g$ is the gravitational stress tensor [Eq. (1) of Box 13.4], which resembles the magnetic one:

$$\mathbf{T}_g = -\frac{g^2 \mathbf{g}}{8\pi G} + \frac{\mathbf{g} \otimes \mathbf{g}}{4\pi G} \, ; \tag{19.13}$$

it is generally unimportant in laboratory plasmas but can be quite important in some astrophysical plasmas — e.g., near black holes and neutron stars.

The two terms in the magnetic Maxwell stress tensor, Eq. (19.11) can be identified as the "push" of an isotropic magnetic pressure of $B^2/2\mu_0$ that acts just like the gas pressure P,

and the "pull" of a tension B^2/μ_0 that acts parallel to the magnetic field. The combination of the tension and the isotropic pressure give *a net tension $B^2/2\mu_0$ along the field and a net pressure $B^2/2\mu_0$ perpendicular to the field lines* (Ex. 1.14).

The magnetic force density

$$\mathbf{f}_m = -\boldsymbol{\nabla}\cdot\mathbf{T}_M = \mathbf{j}\times\mathbf{B} = \frac{(\boldsymbol{\nabla}\times\mathbf{B})\times\mathbf{B}}{\mu_o} \tag{19.14}$$

can be rewritten, using standard vector identities, as

$$\boxed{\mathbf{f}_m = -\boldsymbol{\nabla}\left(\frac{B^2}{2\mu_0}\right) + \frac{(\mathbf{B}\cdot\nabla)\mathbf{B}}{\mu_0} = -\left[\boldsymbol{\nabla}\left(\frac{B^2}{2\mu_0}\right)\right]_\perp + \left[\frac{(\mathbf{B}\cdot\nabla)\mathbf{B}}{\mu_0}\right]_\perp}. \tag{19.15}$$

Here "$\perp$" means keep only the components perpendicular to the magnetic field; the fact that $\mathbf{f}_m = \mathbf{j}\times\mathbf{B}$ guarantees that the net force parallel to $\mathbf{B}$ must vanish, so we can throw away the component along $\mathbf{B}$ in each term. This transversality of $\mathbf{f}_m$ means that the magnetic force does not inhibit nor promote motion of the fluid along the magnetic field. Instead, fluid elements are free to slide along the field like beads that slide without friction along a magnetic "wire".

The "$\perp$" expressions in Eq. (19.15) say that the magnetic force density has two parts: first, the negative of the two-dimensional gradient of the magnetic pressure $B^2/2\mu_0$ orthogonal to $\mathbf{B}$ (Fig. 19.3a), and second, an orthogonal *curvature force* $(\mathbf{B}\cdot\boldsymbol{\nabla})\mathbf{B}/\mu_0$, which has magnitude $B^2/\mu_0 R$, where R is the radius of curvature of a field line. This curvature force acts toward the field line's center of curvature (Fig. 19.3b) and is the magnetic-field-line analog of the force that acts on a curved wire or curved string under tension.

Just as the magnetic force density dominates and the electric force is negligible $[O(v^2/c^2)]$ in our nonrelativistic situation, so also the electromagnetic contribution to the energy density

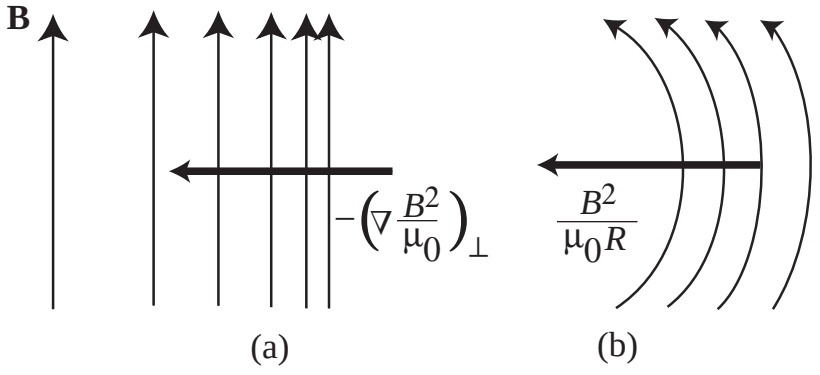

Fig. 19.3: Contributions to the electromagnetic force density acting on a conducting fluid in a non-uniform magnetic field. There is a magnetic-pressure force density $-(\boldsymbol{\nabla}B^2/2\mu_0)_\perp$ acting perpendicular to the field. And there is a magnetic-curvature force density $[(\mathbf{B}\cdot\boldsymbol{\nabla})\mathbf{B}/\mu_0]_\perp$, which is also perpendicular to the magnetic field and lies in the plane of the field's bend, pointing toward its center of curvature; the magnitude of this curvature force density is $(B^2/\mu_0 R)$ where R is the radius of curvature.

is predominantly due to the magnetic term $U_M = B^2/2\mu_0$ with negligible electric contribution. The electromagnetic energy flux is just the Poynting Flux $\mathbf{F}_M = \mathbf{E}\times\mathbf{B}/\mu_0$, with $\mathbf{E}$ given by Eq. (19.5b). Inserting these into the law of energy conservation (13.58) (and continuing to neglect viscosity), we obtain

$$\frac{\partial}{\partial t}\left[\left(\frac{1}{2}v^2 + u + \Phi\right)\rho + \frac{B^2}{2\mu_0}\right] + \nabla\cdot\left[(\frac{1}{2}v^2 + h + \Phi)\rho\mathbf{v} + \frac{\mathbf{E}\times\mathbf{B}}{\mu_0}\right] = 0\ . \tag{19.16}$$

When gravitational energy is important, we must augment this equation with the gravitational energy density and flux, as discussed in Box 13.4.

As in Sec. 13.7.4, we can combine this energy conservation law with mass conservation and the first law of thermodynamics to obtain an equation for the evolution of entropy: Eqs. (13.75) and (13.76) are modified to read

$$\boxed{\frac{\partial(\rho s)}{\partial t} + \nabla\cdot(\rho s\mathbf{v}) = \rho\frac{ds}{dt} = \frac{j^2}{\kappa_e T}}\ . \tag{19.17}$$

Thus, just as viscosity increases entropy through viscous dissipation, and thermal conductivity increases entropy through diffusive heat flow [Eqs. (13.75) and (13.76)], so also electrical conductivity increases entropy through Ohmic dissipation. From Eq. (19.17) we see that our fourth transport coefficient κ_e, like our previous three (the two coefficients of viscosity $\eta \equiv \rho\nu$ and ζ and the thermal conductivity κ), is constrained to be positive by the second law of thermodynamics.

****

EXERCISES

Exercise 19.1 *Derivation: Basic Equations of MHD*

(a) Verify that $-\boldsymbol{\nabla}\cdot\mathbf{T}_M = \mathbf{j}\times\mathbf{B}$ where $\mathbf{T}_M$ is the magnetic stress tensor (19.11).

(b) Take the scalar product of the fluid velocity $\mathbf{v}$ with the equation of motion (19.10) and combine with mass conservation to obtain the energy conservation equation (19.16).

(c) Combine energy conservation (19.16) with the first law of thermodynamics and mass conservation to obtain Eq. (19.17) for the evolution of the entropy.

****

19.2.3 Boundary Conditions

The equations of MHD must be supplemented by boundary conditions at two different types of interfaces. The first is a *contact discontinuity*, i.e. the interface between two distinct media that do not mix; for example the surface of a liquid metal or a rigid wall of a plasma

containment device. The second is a *shock front* which is being crossed by the fluid. Here the boundary is between shocked and unshocked fluid.

We can derive the boundary conditions by transforming into a primed frame in which the interface is instantaneously at rest (not to be confused with the fluid's local rest frame) and then transforming back into our original unprimed inertial frame. In the primed frame, we resolve the velocity and magnetic and electric vectors into components normal and tangential to the surface. If $\mathbf{n}$ is a unit vector normal to the surface, then the normal and tangential components of velocity in either frame are

$$v_n = \mathbf{n}\cdot\mathbf{v}\ , \quad \mathbf{v}_t = \mathbf{v} - (\mathbf{n}\cdot\mathbf{v})\mathbf{n}\ , \tag{19.18}$$

and similarly for the $\mathbf{E}$ and $\mathbf{B}$. *At a contact discontinuity,*

$$\boxed{v'_n = v_n - v_{sn} = 0} \tag{19.19a}$$

on both sides of the interface surface; here v_{sn} is the normal velocity of the surface. *At a shock front,* mass flux across the surface is conserved [cf. Eq. (17.29a)]:

$$\boxed{[\rho v'_n] = [\rho(v_n - v_{sn})] = 0}\ . \tag{19.19b}$$

Here, as in Sec. 17.5, we use the notation $[X]$ to signify the difference in some quantity X across the interface.

When we consider the magnetic field, it does not matter which frame we use since $\mathbf{B}$ is unchanged to the Galilean order at which we are working. Let us construct a thin "pill box" $\mathcal{V}$ (Fig. 19.4) and integrate the equation $\boldsymbol{\nabla}\cdot\mathbf{B} = 0$ over its volume, invoke the divergence theorem and let the box thickness diminish to zero; thereby we see that

$$\boxed{[B_n] = 0}\ . \tag{19.19c}$$

By contrast, the tangential component of the magnetic field can be discontinuous across an interface because of surface currents: by integrating $\boldsymbol{\nabla}\times\mathbf{B} = \mu_0\mathbf{j}$ across the shock front, we can deduce that

$$\boxed{[\mathbf{B}_t] = \mu_0\mathbf{n}\times\mathbf{J}}\ , \tag{19.19d}$$

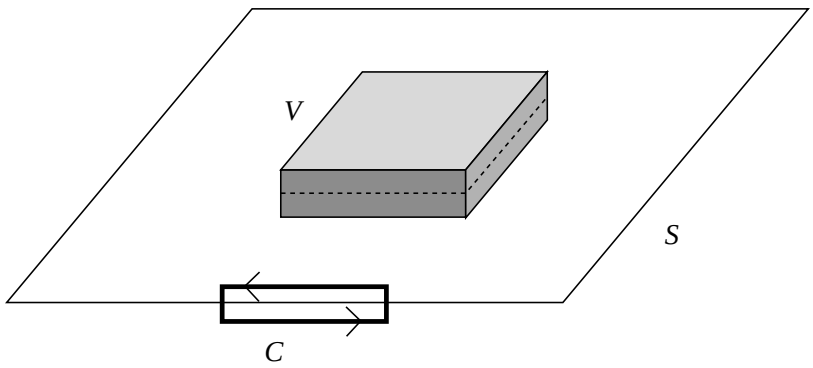

Fig. 19.4: (a) Elementary pill box $\mathcal{V}$ and (b) elementary circuit $\mathcal{C}$ used in deriving the MHD junction conditions at a surface S.

where $\mathbf{J}$ s the surface current density.

We deduce the boundary condition on the electric field by integrating Maxwell's equation $\boldsymbol{\nabla}\times\mathbf{E} = -\partial\mathbf{B}/\partial t$ over the area bounded by the circuit $\mathcal{C}$ in Fig. 19.4 and using Stokes theorem, letting the two short legs of the circuit vanish. We thereby obtain

$$\boxed{[\mathbf{E}'_t] = [\mathbf{E}_t] + [(\mathbf{v}_s\times\mathbf{B})_t] = 0}\,, \tag{19.19e}$$

where $\mathbf{v}_s$ is the velocity of a frame that moves with the surface. Note that only the normal component of the velocity contributes to this expression, so we can replace $\mathbf{v}_s$ by $v_{sn}\mathbf{n}$. The normal component of the electric field, like the tangential component of the magnetic field, can be discontinuous as there may be surface charge at the interface.

There are also dynamical boundary conditions that can be deduced by integrating the laws of momentum conservation (19.12) and energy conservation (19.16) over the pill box and using Gauss's theorem to convert the volume integral of a divergence to a surface integral. The results, naturally, are the requirements that the normal fluxes of momentum $\mathbf{T}\cdot\mathbf{n}$ and energy $\mathbf{F}\cdot\mathbf{n}$ be continuous across the surface [$\mathbf{T}$ being the total stress, i.e., the quantity inside the divergence in Eq. (19.12) and $\mathbf{F}$ the total energy flux, i.e., the quantity inside the divergence in Eq. (19.16)]; see Eqs. (17.30) and (17.31) and associated discussion. The normal and tangential components of $[\mathbf{T}\cdot\mathbf{n}] = 0$ read

$$\boxed{\left[P + \rho(v_n - v_{sn})^2 + \frac{B_t^2}{2\mu_0}\right] = 0}\,, \tag{19.19f}$$

$$\boxed{\left[\rho(v_n - v_{sn})(\mathbf{v}_t - \mathbf{v}_{st}) - \frac{B_n\mathbf{B}_t}{\mu_0}\right] = 0}\,, \tag{19.19g}$$

where we have omitted the gravitational stress, since it will always be continuous in situations studied in this chapter (no surface layers of mass). Similarly, continuity of the energy flux $[\mathbf{F}\cdot\mathbf{n}] = 0$ reads

$$\boxed{\left[\left(\frac{1}{2}v^2 + h + \Phi\right)\rho(v_n - v_{sn}) + \frac{\mathbf{n}\cdot[(\mathbf{E}+\mathbf{v}_s\times\mathbf{B})\times\mathbf{B}]}{\mu_0}\right] = 0}\,. \tag{19.19h}$$

When the interface has plasma on one side and a vacuum magnetic field on the other, as in devices for magnetic confinement of plasmas (Sec. 19.3 below), the vacuum electromagnetic field, like that in the plasma, has small time derivatives: $\partial/\partial t \sim v\partial/\partial x^j$. As a result, the vacuum displacement current $\epsilon_0\partial\mathbf{E}/\partial t$ is very small, and the vacuum Maxwell equations reduce to the same form as those in the MHD plasma, but with ρ_e and $\mathbf{j}$ zero. As a result, the boundary conditions at the vacuum-plasma interface (Ex. 19.2) are those discussed above, but with ρ and P vanishing on the vacuum side.

****

EXERCISES

Exercise 19.2 *Example and Derivation: Perfect MHD Boundary Conditions at a Fluid-Vacuum Interface*
In analyzing the stability of configurations for magnetic confinement of a plasma (Sec. 19.5), one needs boundary conditions at the plasma-vacuum interface, for the special case of perfect MHD (electrical conductivity idealized as arbitrarily large). Denote by a tilde, $\tilde{\mathbf{B}}$ and $\tilde{\mathbf{E}}$, the magnetic and electric fields in the vacuum, and reserve non-tilde symbols for quantities on the plasma side of the interface.

(a) Show that the normal-force boundary condition (19.19f) reduces to an equation for the vacuum region's tangential magnetic field:

$$\frac{\tilde{B}_t^2}{2\mu_0} = P + \frac{B_t^2}{2\mu_0} \ . \tag{19.20a}$$

(b) By combining Eqs. (19.19c) and (19.19g) and noting that $v_n - v_{sn}$ must vanish (why?), show that, for magnetic confinement the normal component of the magnetic field must vanish on both sides of the interface:

$$\tilde{B}_n = B_n = 0 \ . \tag{19.20b}$$

(c) In analyzing energy flow across the interface, it is necessary to know the tangential electric field. On the plasma side, $\tilde{\mathbf{E}}_t$ is a secondary quantify fixed by projecting tangentially the relation $\mathbf{E} + \mathbf{v} \times \mathbf{B} = 0$. On the vacuum side it is fixed by the boundary condition (19.19e). By combining these two relations, show that

$$\tilde{E}_t + \mathbf{v}_{sn} \times \tilde{B}_t = 0 \ . \tag{19.20c}$$

Exercise 19.3 *Problem: Diffusion of Magnetic Field*
Consider an infinitely long cylinder of plasma with constant electric conductivity, surrounded by vacuum. Assume that the cylinder initially is magnetized uniformly parallel to its length, and assume that the field decays quickly enough that the plasma's inertia keeps it from moving much during the decay (so $\mathbf{v} \simeq 0$).

(a) Show that the reduction of magnetic energy as the field decays is compensated by the Ohmic heating of the plasma plus energy lost to outgoing electromagnetic waves (which will be negligible if the decay is slow).

(b) Compute the approximate magnetic profile after the field has decayed to a small fraction of its original value. Your answer should be expressible in terms of a Bessel function.

Exercise 19.4 *Example: Shock with Transverse Magnetic Field*
Consider a normal shock wave ($\mathbf{v}$ perpendicular to the shock front), in which the magnetic field is parallel to the shock front, analyzed in the shock front's rest frame.

(a) Show that the junction conditions across the shock are

$$[\rho v] = [P + \rho v^2 + B^2/2\mu_0] = [h + v^2/2 + B^2/\mu_0\rho] = [vB] = 0 \ . \tag{19.21}$$

(b) Specialize to a fluid with equation of state $P \propto \rho^\gamma$. Show that these junction conditions predict no compression, $[\rho] = 0$, if the upstream velocity is $v_1 = C_f \equiv \sqrt{(B_1^2/\mu_0 + \gamma P_1)/\rho_1}$. For v_1 greater than this C_f, the fluid gets compressed.

(c) Explain why this means that the speed of sound perpendicular to the magnetic field must be C_f. As we shall see in Sec. 19.7.2, this indeed is the case: C_f is the speed (19.76) of a *fast magnetosonic wave*, the only kind of sound wave that can propate perpendicular to **B**.

Exercise 19.5 *Problem: The Earth's Bow Shock*
The solar wind is a supersonic, hydromagnetic flow of plasma originating in the solar corona. At the radius of the earth's orbit, the wind's density is $\rho \sim 6 \times 10^{-21}$ kg m^{-3}, its velocity is $v \sim 400$ km s^{-1}, its temperature is $T \sim 10^5$ K and its magnetic field strength is $B \sim 1$ nT.

(a) By balancing the wind's momentum flux with the magnetic pressure exerted by the earth's dipole magnetic field, estimate the radius above the earth at which the solar wind passes through a bow shock (Fig. 17.2).

(b) Consider a strong perpendicular shock at which the magnetic field is parallel to the shock front. Show that the magnetic field strength will increase by the same ratio as the density, when crossing the shock front. Do you expect the compression to increase or decrease as the strength of the field is increased, keeping all of the other flow variables constant?

****

19.2.4 Magnetic field and vorticity

We have already remarked on how the magnetic field and the vorticity are both axial vectors that can be written as the curl of a polar vector and that they satisfy similar transport equations. It is not surprising that they are physically intimately related. To explore this relationship in full detail would take us beyond the scope of this book. However, we can illustrate their interaction by showing how they can create each other. In brief: *vorticity can twist a magnetic field, amplifying it; and an already twisted field, trying to untwist itself, can create vorticity.* In greater detail:

First, consider a simple vortex through which passes a uniform magnetic field (Fig. 19.2a above). If the magnetic Reynolds number is large enough, then the magnetic field will be carried with the flow and get wound up like spaghetti on the end of a fork (Fig. 19.2b, continued for a longer time). This will increase the magnetic energy in the vortex, though not the mean flux of magnetic field. This amplification will continue until either the field

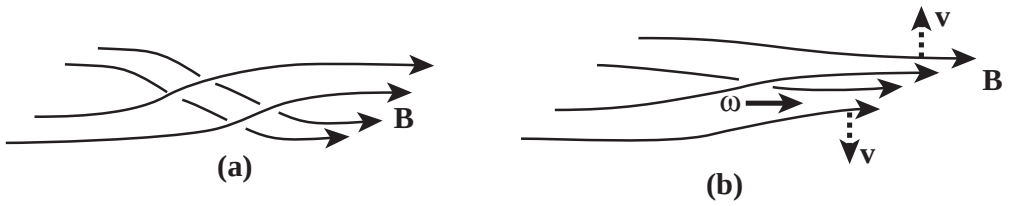

Fig. 19.5: When a twisted magnetic field is frozen into an irrotational flow as in (a), the field will try to untwist and in the process will create vorticity as in (b).

gradient is large enough that the field decays through Ohmic dissipation, or the field strength is large enough to react back on the flow and stop it spinning.

Second, consider an irrotational flow containing a twisted magnetic field (Fig. 19.5a). Provided that the magnetic Reynolds number is sufficiently large, the magnetic stress, attempting to untwist the field, will act on the flow and induce vorticity (Fig. 19.5b). We can describe this formally by taking the curl of the equation of motion (19.10). Assuming, for simplicity, that the density ρ is constant and the electric conductivity is infinite, we obtain

$$\frac{\partial \boldsymbol{\omega}}{\partial t} - \boldsymbol{\nabla} \times (\mathbf{v} \times \boldsymbol{\omega}) = \frac{\boldsymbol{\nabla} \times [(\boldsymbol{\nabla} \times \mathbf{B}) \times \mathbf{B}]}{\mu_0 \rho} \,. \tag{19.22}$$

The term on the right-hand side of this equation changes the number of vortex lines threading the fluid, just like the $\boldsymbol{\nabla} P \times \boldsymbol{\nabla} \rho / \rho^2$ term on the right-hand side of Eq. (14.3). Note, however, that because the divergence of the vorticity is zero, any fresh vortex lines that are made must be created as continuous curves that grow out of points or lines where the vorticity vanishes.

19.3 Magnetostatic Equilibria

19.3.1 Controlled thermonuclear fusion

For more than a half century, plasma physicists have striven to release nuclear energy in a controlled manner by confining plasma at a temperature in excess of a hundred million degrees using strong magnetic fields. In the most widely studied scheme, deuterium and tritium combine according to the reaction

$$\mathrm{d} + \mathrm{t} \rightarrow \alpha + \mathrm{n} + 22.4\mathrm{MeV}. \tag{19.23}$$

The fast neutrons can be absorbed in a surrounding blanket of lithium and the heat can then be used to drive a generator.

At first this task seemed quite simple. However, it eventually became clear that it is very difficult to confine hot plasma with a magnetic field because most confinement geometries are unstable. In this book we shall restrict our attention to a few simple confinement devices, emphasizing the one that is the basis of most modern efforts, the *Tokamak*. (Tokamaks were originally developed in the Soviet Union and the word is derived from a Russian abbreviation for toroidal magnetic field.) In this section, we shall treat equilibrium configurations; in Sec. 19.4, we shall consider their stability.

In our discussions of both equilibrium and stability, we shall treat the plasma in the MHD approximation. At first this might seem rather unrealistic, because we are dealing with a dilute gas of ions and electrons that undergo infrequent Coulomb collisions. However, as we shall discuss in Sec. 20.5.1 and justify in Chaps. 22 and 23, collective effects produce a sufficiently high effective collision frequency to make the plasma behave like a fluid, so MHD is usually a good approximation for describing these equilibria and their rather slow temporal evolution.

Let us examine some numbers that characterize the regime in which a successful controlled-fusion device must operate.

The ratio of plasma pressure to magnetic pressure

$$\boxed{\beta \equiv \frac{P}{B^2/2\mu_0}} \tag{19.24}$$

plays a key role. For the magnetic field to have any chance of confining the plasma, its pressure must exceed that of the plasma; i.e., β must be less than one. The most successful designs achieve $\beta \sim 0.2$. The largest field strengths that can be safely sustained in the laboratory are $B \sim 10$ T $= 100$ kG, so $\beta \lesssim 0.2$ limits the gas pressure to $P \lesssim 10^7$ Pa ~ 100 atmospheres.

Plasma fusion can only be economically feasible if more power is released by nuclear reactions than is lost to radiative cooling. Both heating and cooling are proportional to the square of the number density of hydrogen ions, n^2. However, while the radiative cooling rate increases comparatively slowly with temperature, the nuclear reaction rate increases very rapidly. (This is because, as the mean energy of the ions increases, the number of ions in the Maxwellian tail of the distribution function that are energetic enough to penetrate the Coulomb barrier increases exponentially). This means that, in order for the rate of heat production to greatly exceed the rate of cooling, the temperature need only be modestly higher than that for them to be equal—which is a minimum temperature essentially fixed by atomic and nuclear physics. In the case of a d-t plasma this is $T_{\rm min} \sim 10^8$ K. The maximum hydrogen density that can be confined is therefore $n_{\rm max} = P/2kT_{\rm min} \sim 3 \times 10^{21}$ m^{-3}. (The Factor 2 comes from the electrons, which produce the same pressure as the ions.)

Now, if a volume V of plasma is confined at a given number density n and temperature $T_{\rm min}$ for a time τ, then the amount of nuclear energy generated will be proportional to $n^2V\tau$, while the energy to heat the plasma up to $T_{\rm min}$ is $\propto nV$. Therefore, there is a minimum value of the product $n\tau$ that must be attained before there will be net energy production. This condition is known as the *Lawson criterion*. Numerically, the plasma must be confined for

$$\tau \sim (n/10^{20}{\rm m}^{-3})^{-1}\ {\rm s}, \tag{19.25}$$

typically ~ 30 ms. Now the sound speed at these temperatures is $\sim 3 \times 10^5$ m s^{-1} and so an unconfined plasma would hit the few-meter-sized walls of the vessel in which it is held in a few μs. Therefore, *the magnetic confinement must be effective for typically* $10^4 - 10^5$ *dynamical timescales (sound crossing times).* It is necessary that the plasma be confined and confined well if we want to build a viable fusion reactor.

19.3.2 Z-Pinch

Before discussing plasma confinement by Tokamaks, we shall describe a simpler confinement geometry known as the *Z-pinch* (Fig. 19.6a). In a Z-pinch, electric current is induced to flow along a cylinder of plasma. This current creates a toroidal magnetic field whose tension prevents the plasma from expanding radially much like hoops on a barrel prevent it from exploding. Let us assume that the cylinder has a radius R and is surrounded by vacuum.

Now, in static equilibrium we must balance the plasma pressure gradient by a Lorentz force:

$$\boldsymbol{\nabla} P = \mathbf{j} \times \mathbf{B} \; . \tag{19.26}$$

(Gravitational forces can safely be ignored.) Equation (19.26) implies immediately that $\mathbf{B} \cdot \boldsymbol{\nabla} P = \mathbf{j} \cdot \boldsymbol{\nabla} P = 0$, so both the magnetic field and the current density lie on constant pressure (or *isobaric*) surfaces. An equivalent version of the force balance equation (19.26), obtained using Eq. (19.15), says

$$\frac{d}{d\varpi}\left(P + \frac{B^2}{2\mu_0}\right) = -\frac{B^2}{\mu_0 \varpi} \; , \tag{19.27}$$

where ϖ is the radial cylindrical coordinate. This exhibits the balance between the gradient of plasma and magnetic pressure on the left, and the magnetic tension (the "hoop force") on the right. Treating this as a differential equation for B^2 and integrating it assuming that P falls to zero at the surface of the column, we obtain for the surface magnetic field

$$B^2(R) = \frac{4\mu_0}{R^2} \int_0^R P \varpi d\varpi \; . \tag{19.28}$$

We can re-express the surface toroidal field in terms of the total current flowing along the plasma as $B(R) = \mu_0 I / 2\pi R$ (Ampere's law); and assuming that the plasma is primarily hydrogen so its ion density n and electron density are equal, we can write the pressure as $P = 2nk_BT$. Inserting these into Eq. (19.28), integrating and solving for the current, we obtain

$$I = \left(\frac{16\pi N k_B T}{\mu_0}\right)^{1/2} \; , \tag{19.29}$$

where N is the number of ions per unit length. For a 1 m column of plasma with hydrogen density $n \sim 10^{20}$ m^{-3} and temperature $T \sim 10^8$ K, this says that currents of several MA are required for confinement.

19.3.3 Θ-Pinch

There is a complementary equilibrium for a cylindrical plasma, in which the magnetic field lies parallel to the axis and the current density encircles the cylinder (Fig. 19.6b). This is called the *θ-pinch*. This configuration is usually established by making a cylindrical metal tube with a small gap so that current can flow around it as shown in the figure. The tube is filled with cold plasma and then the current is turned on quickly, producing a quickly growing longitudinal field inside the tube (as inside a solenoid). Since the plasma is highly

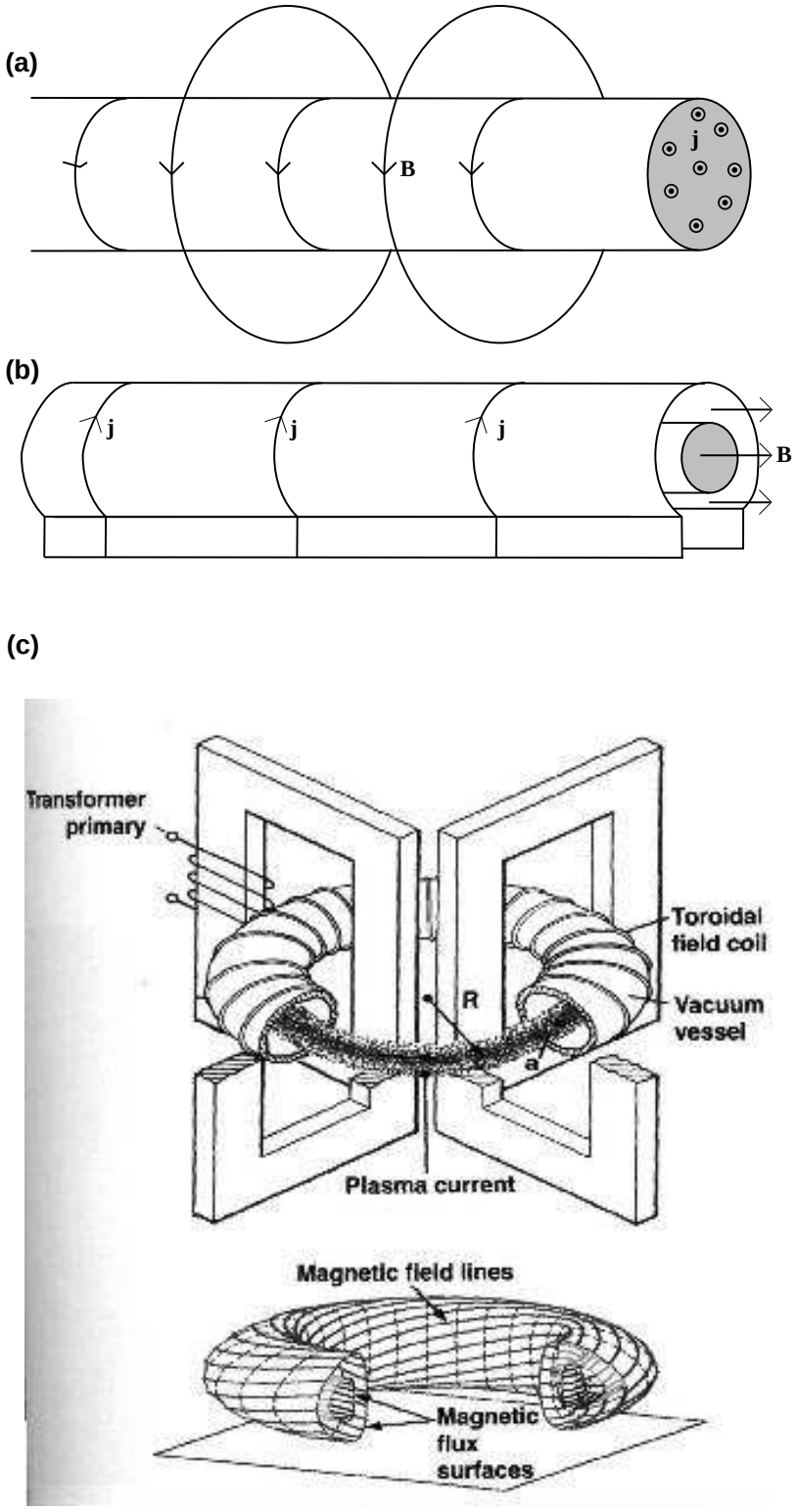

Fig. 19.6: (a) The Z-pinch. (b) The θ-pinch. (c) The Tokamak.

conducting, the field lines cannot penetrate the plasma column but instead exert a pressure on its surface causing it to shrink radially and rapidly. The plasma heats up due to both the radial work done on it and Ohmic heating. Equilibrium is established when the plasma's pressure P balances the magnetic pressure $B^2/2\mu_0$ at the plasma's surface.

19.3.4 Tokamak

One of the problems with these pinches (and we shall find other problems below!) is that they have ends through which plasma can escape. This is readily cured by replacing the cylinder with a torus. The most stable geometry, called the *Tokamak*, combines features of both Z- and θ-pinches; see Fig. 19.6c. If we introduce spherical coordinates (r, θ, ϕ), then magnetic field lines and currents that lie in an r, θ plane (orthogonal to $\vec{e}_\phi$) are called *poloidal*, whereas their ϕ components are called *toroidal*. In a Tokamak, the toroidal magnetic field is created by external poloidal current windings. However, the poloidal field is mostly created as a consequence of toroidal current induced to flow within the plasma torus. The resulting net field lines wrap around the plasma torus in a helical manner, defining a magnetic surface on which the pressure is constant. The average value of $2\pi d\theta/d\phi$ along the trajectory of a field line is called the rotational transform, ι, and is a property of the magnetic surface on which the field line resides. If $\iota/2\pi$ is a rational number, then the field line will close after a finite number of circuits. However, in general, $\iota/2\pi$ will not be rational so a single field line will cover the whole magnetic surface ergodically. This allows the plasma to spread over the whole surface rapidly. The rotational transform is a measure of the toroidal current flowing within the magnetic surface and of course increases as we move outwards from the innermost magnetic surface, while the pressure decreases.

The best performance as of 2013 was registered by the Joint European Torus (JET) in the UK in 1997 (see Keilhacker et. al. (1998)]. The radius of the torus was ~ 3.0 m, the magnetic field strength was $B \sim 3.5$ T, and the fuel was a 50/50 mixture of deuterium and tritium. A nuclear power output of ~ 16 MW was produced with ~ 25 MW of input heating. The confinement time was $\tau \sim 1$ s.

The next major step is ITER (whose name means "the way" in Latin): a Tokamak-based experimental fusion reactor being constructed by a large international consortium; see `http://www.iter.org/`. Its Tokamak will be about twice as large in linear dimensions as JET and its goal is a fusion power output of 410 MW.

Even when "break-even" (nuclear power out equal to heating power in), with large output power, can be attained routinely, there will remain major engineering problems before controlled fusion will be fully practical.

****

EXERCISES

Exercise 19.6 *Problem: Strength of Magnetic Field in a Magnetic Confinement Device*
The currents that are sources for strong magnetic fields have to be held in place by solid conductors. Estimate the limiting field that can be sustained using normal construction materials.

Exercise 19.7 *Problem: Force-free Equilibria*
In an equilibrium state of a very low-β plasma, the plasma's pressure force density $-\boldsymbol{\nabla}P$ is ignorably small and so the Lorentz force density $\mathbf{j}\times\mathbf{B}$ must vanish [Eq. (19.10)]. Such a plasma is said to be "force-free". This, in turn, implies that the current density is parallel to the magnetic field, so $\boldsymbol{\nabla}\times\mathbf{B}=\alpha\mathbf{B}$. Show that α must be constant along a field line, and that if the field lines eventually travel everywhere, then α must be constant everywhere.

****

19.4 Hydromagnetic Flows

We now introduce fluid motions into our applications of magnetohydrodyanmics. Specifically, we explore a simple class of *stationary hydromagnetic flows*: the flow of an electrically conducting fluid along a duct of constant cross-section perpendicular to a uniform magnetic field B_0 (see Fig. 19.7). This is sometimes known as *Hartmann Flow*. The duct has two insulating walls (top and bottom as shown in the figure), separated by a distance $2a$ that is much smaller than the separation of short side walls, which are electrically conducting.

In order to relate Hartmann flow to magnetic-free Poiseuille flow (viscous, laminar flow between plates; Ex. 13.18), we shall reinstate the viscous force in the equation of motion. For simplicity we shall assume that the time-independent flow ($\partial\mathbf{v}/\partial t=0$) has travelled sufficiently far down the duct (z direction) to have reached a z-independent form, so $\mathbf{v}\cdot\boldsymbol{\nabla}\mathbf{v}=0$ and $\mathbf{v}=\mathbf{v}(x,y)$; and we assume that gravitational forces are unimportant. Then the flow's equation of motion takes the form

$$\boldsymbol{\nabla}P=\mathbf{j}\times\mathbf{B}+\eta\nabla^2\mathbf{v}\ , \tag{19.30}$$

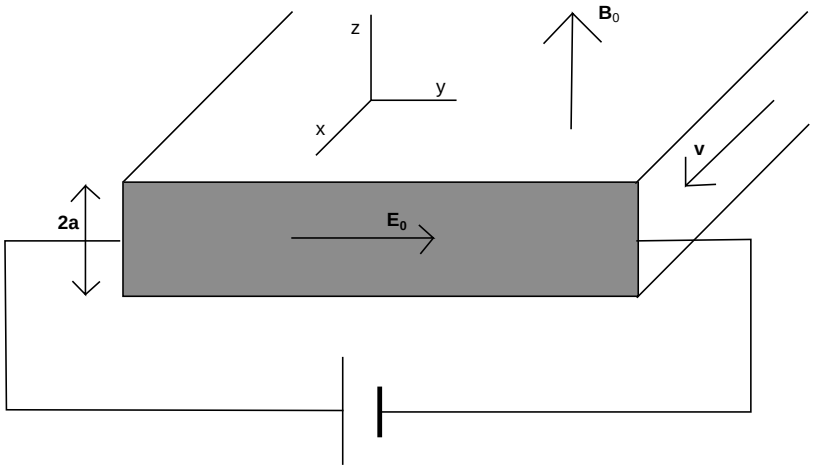

Fig. 19.7: Hartmann flow with average speed v along a duct of thickness $2a$, perpendicular to an applied magnetic field of strength B_0. The short side walls are conducting and the two long horizontal walls are electrically insulating.

where $\eta = \rho\nu$ is the coefficient of dynamical viscosity. The magnetic (Lorentz) force $\mathbf{j}\times\mathbf{B}$ will alter the balance between the Poiseuille flow's viscous force $\eta\nabla^2\mathbf{v}$ and the pressure gradient $\boldsymbol{\nabla}P$. The details of that altered balance and the resulting magnetic-influenced flow will depend on how the walls are connected electrically. Let us consider four possibilities that bring out the essential physics:

Electromagnetic Brake; Fig. 19.8a

We short circuit the electrodes so a current $\mathbf{j}$ can flow. The magnetic field lines are partially dragged by the fluid, bending them (as embodied in $\boldsymbol{\nabla}\times\mathbf{B} = \mu_0\mathbf{j}$) so they can exert a decelerating tension force $\mathbf{j}\times\mathbf{B} = (\boldsymbol{\nabla}\times\mathbf{B})\times\mathbf{B}/\mu_0 = \mathbf{B}\cdot\boldsymbol{\nabla}\mathbf{B}/\mu_0$ on the flow (Fig. 19.3b). This is an *Electromagnetic Brake*. The pressure gradient, which is trying to accelerate the fluid, is balanced by the magnetic tension and viscosity. The work being done (per unit volume) by the pressure gradient, $\mathbf{v}\cdot(-\boldsymbol{\nabla}P)$, is converted into heat through viscous and Ohmic dissipation.

MHD Power generator; Fig. 19.8b

This is similar to the electromagnetic brake except that an external load is added to the circuit. Useful power can be extracted from the flow. Variants of this were developed in the 1970s–1990s in many countries, but interest in them is currently (2013) in decline, as they are not now economically competitive with other power-generation methods. [ROGER: IS THIS A FAIR STATEMENT? - KIP]

Flow Meter; Fig. 19.8c

When the electrodes are on open circuit, the induced electric field will produce a measurable potential difference across the duct. This voltage will increase monotonically with the rate of flow of fluid through the duct and therefore can provide a measurement of the flow.

Electromagnetic Pump; Figs. 19.7 and 19.8d

Finally we can attach a battery to the electrodes and allow a current to flow. This produces a Lorentz force which either accelerates or decelerates the flow depending on the

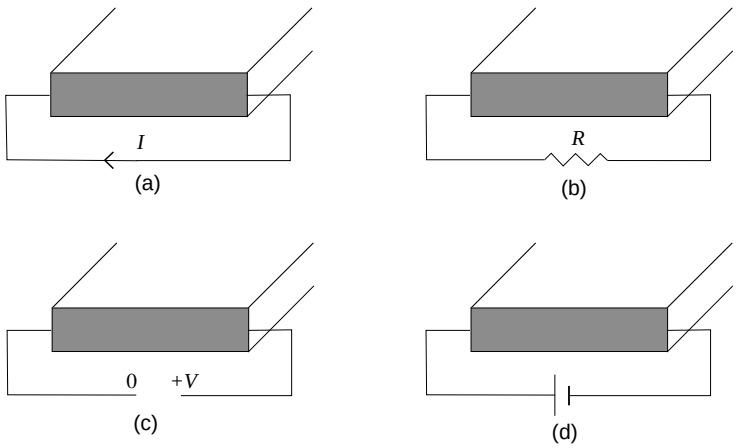

Fig. 19.8: Four variations on Hartmann flow: a)Electromagnetic Brake. b) MHD Power generator. c) Flow meter. d) Electromagnetic pump.

direction of the magnetic field. This method is used to pump liquid sodium coolant around a nuclear reactor. It has also been proposed as a means of spacecraft propulsion in interplanetary space.

We consider in some detail two limiting cases of the electromagnetic pump. When there is a constant pressure gradient $Q = -dP/dx$ but no magnetic field, a flow with modest Reynolds number will be approximately laminar with velocity profile (Ex. 13.18)

$$v_z(y) = \frac{Qa^2}{2\eta}\left[1 - \left(\frac{y}{a}\right)^2\right] , \tag{19.31}$$

where a is the half width of the channel. This is the one-dimensional version of the "Poiseuille flow" in a pipe such as a blood artery, which we studied in Sec. 13.7.6; cf. Eq. (13.82a). Now suppose that uniform electric and magnetic fields E_0, B_0 are applied along the $\mathbf{e}_x$ and $\mathbf{e}_y$ directions respectively (Fig. 19.7). The resulting magnetic force $\mathbf{j}\times\mathbf{B}$ can either reinforce or oppose the fluid's motion. When the applied magnetic field is small, $B_0 \ll E_0/v_z$, the effect of the magnetic force will be very similar to that of the pressure gradient, and Eq. 19.31 must be modified by replacing $Q \equiv -dP/dz$ by $-dP/dz + j_x B_y = -dP/dz + \kappa_e E_0 B_0$. [Here $j_x = \kappa_e(E_x - v_z B_y) \simeq \kappa_e E_0$.]

If the strength of the magnetic field is increased sufficiently, then the magnetic force will dominate the viscous force, except in thin boundary layers near the walls. Outside the boundary layers, in the bulk of the flow, the velocity will adjust so that the electric field vanishes in the rest frame of the fluid, i.e. $v_z = E_0/B_0$. In the boundary layers there will be a sharp drop of v_z from E_0/B_0 to zero at the walls, and correspondingly a strong viscous force, $\eta\nabla^2\mathbf{v}$. Since the pressure gradient $\boldsymbol{\nabla}P$ must be essentially the same in the boundary layer as in the adjacent bulk flow and thus cannot balance this large viscous force, it must be balanced instead by the magnetic force, $\mathbf{j}\times\mathbf{B} + \eta\nabla^2\mathbf{v} = 0$ [Eq. (19.30)] with $\mathbf{j} = \kappa_e(\mathbf{E} + \mathbf{v}\times\mathbf{B}) \sim \kappa_e v_z B_0 \mathbf{e}_x$. We thereby see that the thickness of the boundary layer will be given by

$$\delta_H \sim \left(\frac{\eta}{\kappa_e B^2}\right)^{1/2} . \tag{19.32}$$

This suggests a new dimensionless number to characterize the flow,

$$\boxed{\mathrm{Ha} = \frac{a}{\delta_H} = B_0 a\left(\frac{\kappa_e}{\eta}\right)^{1/2}}, \tag{19.33}$$

called the Hartmann number. The square of the Hartmann number, Ha^2, is essentially the ratio of the magnetic force $|\mathbf{j}\times\mathbf{B}| \sim \kappa_e v_z B_0^2$ to the viscous force $\sim \eta v_z/a^2$, assuming a lengthscale a rather than δ_H for variations of the velocity.

The detailed velocity profile $v_z(y)$ away from the vertical side walls is computed in Exercise 19.8 and is shown for low and high Hartmann numbers in Fig. 19.9. Notice that at low Ha, the plotted profile is nearly parabolic as expected, and at high Ha it consists of boundary layers at $y \sim -a$ and $y \sim a$, and a uniform flow in between.

In Exs. 19.9 and 19.10, we explore two important astrophysical examples of hydromagnetic flow: the magnetosphere of a rotating, magnetized star or other body, and the solar wind.

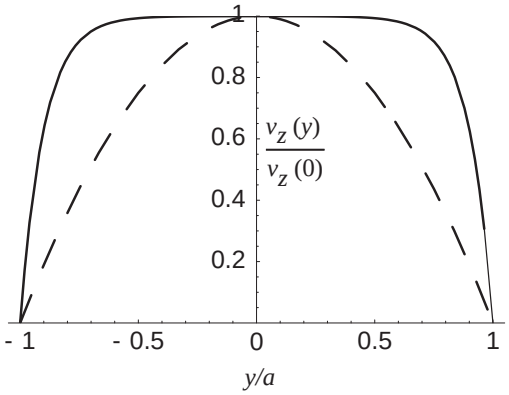

Fig. 19.9: Velocity profiles [Eq. (19.35)] for flow in an electromagnetic pump of width $2a$ with small and large Hartmann number scaled to the velocity at the center of the channel. Dashed curve: the almost parabolic profile for $H = 0.1$ [Eq. (19.31)]. Solid curve: the almost flat topped profile for $H = 10$.

****

EXERCISES

Exercise 19.8 *Example: Hartmann Flow*
Compute the velocity profile of a conducting fluid in a duct of thickness $2a$ perpendicular to externally generated, uniform electric and magnetic fields ($E_0\mathbf{e}_x$ and $B_0\mathbf{e}_y$) as shown in Fig. 19.7. Away from the vertical sides of the duct, the velocity v_z is just a function of y and the pressure can be written in the form $P = -Qz + P(y)$, where Q is the longitudinal pressure gradient.

(a) Show that the velocity field satisfies the differential equation

$$\frac{d^2v_z}{dy^2} - \frac{\kappa_e B_0^2}{\eta} v_z = -\frac{(Q + \kappa_e B_0 E_0)}{\eta} \ . \tag{19.34}$$

(b) Impose suitable boundary conditions at the bottom and top walls of the channel and solve this differential equation to obtain the following velocity field:

$$v_z = \frac{Q + \kappa_e B_0 E_0}{\kappa_e B_0^2} \left[1 - \frac{\cosh(\mathrm{Ha}\, y/a)}{\cosh(\mathrm{Ha})}\right] \ , \tag{19.35}$$

where H is the Hartmann number; cf. Fig. 19.9.

Exercise 19.9 ***Example: Rotating Magnetospheres*
Many self-gravitating cosmic bodies are both spinning and magnetized. Examples are the earth, the sun, black holes surrounded by highly conducting accretion disks (which hold a magnetic field on the hole), neutron stars (pulsars), and magnetic white dwarfs. As a consequence of the magnetic field's spin-induced motion, large electric fields are produced

outside the rotating body. The divergence of these electric fields must be balanced by free electric charge, and this implies that the region around the body cannot be vacuum. It is usually filled with plasma and is called a *magnetosphere*. MHD provides a convenient formalism for describing the structure of this magnetosphere. Magnetospheres are found around most planets and stars. Magnetospheres surrounding neutron stars and black holes are believed to be responsible for the emission from pulsars and quasars.

As a model of a rotating magnetosphere, consider a magnetized and infinitely conducting star, spinning with angular frequency Ω_*. Suppose that the magnetic field is stationary and axisymmetric with respect to the spin axis and that the magnetosphere, like the star, is perfectly conducting.

(a) Show that the azimuthal component of the magnetospheric electric field, E_ϕ, must vanish if the magnetic field is to be stationary. Hence show that there exists a function $\mathbf{\Omega}(\mathbf{r})$ which must be parallel to $\mathbf{\Omega}_*$ and satisfy

$$\mathbf{E} = -(\mathbf{\Omega} \times \mathbf{r}) \times \mathbf{B} \; . \tag{19.36}$$

Show that, if the motion of the magnetosphere's conducting fluid is simply a rotation, then its angular velocity must be $\mathbf{\Omega}$.

(b) Use the induction equation (magnetic-field transport law) to show that

$$(\mathbf{B} \cdot \boldsymbol{\nabla})\mathbf{\Omega} = 0 \; . \tag{19.37}$$

(c) Use the boundary condition at the surface of the star to show that the magnetosphere *corotates* with the star, i.e. $\mathbf{\Omega} = \mathbf{\Omega}_*$. This is known as *Ferraro's law of isorotation*.

Exercise 19.10 *Example: Solar Wind*
The solar wind is a magnetized outflow of plasma that emerges from the solar corona. We will make a simple model of it generalizing the results from the last exercise. In this case, the fluid not only rotates with the sun but also moves away from it. We just consider stationary, axisymmetric motion in the equatorial plane and idealize the magnetic field as having the form $B_r(r), B_\phi(r)$. (If this were true at all latitudes, the sun would have to contain magnetic monopoles!)

(a) Use the results from the previous exercise plus the perfect MHD relation, $\mathbf{E} = -\mathbf{v} \times \mathbf{B}$ to argue that the velocity field can be written in the form

$$\mathbf{v} = \frac{\kappa \mathbf{B}}{\rho} + (\mathbf{\Omega} \times \mathbf{r}). \tag{19.38}$$

where κ and $\mathbf{\Omega}$ are constant along a field line. Interpret this relation kinematically.

(b) Resolve the velocity and the magnetic field into radial and azimuthal components, v_r, v_ϕ, B_r, B_ϕ and show that $\rho v_r r^2, B_r r^2$ are constant.

(c) Use the induction equation to show that

$$\frac{v_r}{v_\phi - \Omega r} = \frac{B_r}{B_\phi}. \tag{19.39}$$

(c) Use the equation of motion to show that the specific angular momentum, including both the mechanical and the magnetic contributions,

$$\Lambda = r v_\phi - \frac{r B_r B_\phi}{\mu_0 \rho v_r} \,, \tag{19.40}$$

is constant.

(e) Combine these two relations to argue that

$$v_\phi = \frac{\Omega r [M_A^2 \Lambda / \Omega r^2 - 1]}{M_A^2 - 1} \,, \tag{19.41}$$

where M_A is the Alfvén Mach number. Show that the solar wind must pass through a critical point where its radial speed equals the Alfvén speed.

(f) In the solar wind, this critical point is located at about 20 solar radii. Explain why this implies that, through the action of the solar wind, the sun loses its spin faster than it loses its mass.

(g) In the vicinity of earth, the radial velocity in the solar wind is about 400 km s^{-1} and the mean proton density is about 4×10^6 m^{-3}. Estimate how long it will take the sun to slow down, and comment on your answer. (The mass of the sun is 2×10^{30} kg, its radius is 7×10^8 m and its rotation period is about 25 days.)

****

19.5 Stability of Magnetostatic Equilibria

Having used the MHD equation of motion to analyze some simple flows, we return to the problem of magnetic confinement, and demonstrate a procedure to analyze the stability of the confinement's magnetostatic equilibria. We first perform a straightforward linear perturbation analysis about equilibrium, obtaining an eigenequation for the perturbation's oscillation frequencies ω. For sufficiently simple equilibria, this eigenequation can be solved analytically; but most equilibria are too complex for this, so the eigenequation must be solved numerically or by other approximation techniques. This is rather similar to the task one faces in attempting to solve the Schrödinger equation for multi-electron atoms. It will not be a surprise to learn that variational methods are especially practical and useful, and we shall develop a suitable formalism for them.

We shall develop the perturbation theory, eigenequation, and variational formalism in some detail not only because of their importance for the stability of magnetostatic equilibria, but also because essentially the same techniques (with different equations) are used in studying the stability of other equilibria. One example is the oscillations and stability of stars, in which the magnetic field is unimportant while self gravity is crucial [see, e.g., Chap. 6 of Shapiro and Teukolsky (1983), and Sec. 16.2.4 of this book, on helioseismology]. Another example is the oscillations and stability of elastostatic equilibria, in which $\mathbf{B}$ is absent but shear stresses are important (Secs. 12.3 and 12.4).

19.5.1 Linear Perturbation Theory

Consider a perfectly conducting, isentropic fluid at rest in equilibrium, with pressure gradients that balance magnetic forces—for example, the Z-pinch, θ-pinch, and Tokamak configurations of Fig. 19.6. For simplicity, we shall ignore gravity. (This is usually justified in laboratory situations.) The equation of equilibrium then reduces to

$$\boldsymbol{\nabla} P = \mathbf{j} \times \mathbf{B} \tag{19.42}$$

[Eq. (19.10)].

We now perturb slightly about our chosen equilibrium and ignore the (usually negligible) effects of viscosity and magnetic-field diffusion, so $\eta = \rho\nu \simeq 0$, $\kappa_e \simeq \infty$. It is useful and conventional to describe the perturbations in terms of two different types of quantities: (i) The change in a quantity (e.g. the fluid density) moving with the fluid, which is called a *Lagrangian* perturbation and denoted by the symbol Δ (e.g, the Lagrangian density perturbation $\Delta\rho$). (ii) The change at fixed location in space, which is called an *Eulerian* perturbation and denoted by the symbol δ (e.g, the Eulerian density perturbation $\delta\rho$). The fundamental variable used in the theory is the fluid's *Lagrangian displacement* $\Delta\mathbf{x} \equiv \boldsymbol{\xi}(\mathbf{x}, t)$; i.e. the change in location of a fluid element, moving with the fluid. A fluid element whose location is $\mathbf{x}$ in the unperturbed equilibrium is moved to location $\mathbf{x} + \boldsymbol{\xi}(\mathbf{x}, t)$ by the perturbations. From their definitions, one can see that the Lagrangian and Eulerian perturbations are related by

$$\boxed{\Delta = \delta + \boldsymbol{\xi} \cdot \boldsymbol{\nabla}}\ , \qquad \text{e.g.,} \quad \Delta\rho = \delta\rho + \xi \cdot \boldsymbol{\nabla}\rho\ . \tag{19.43}$$

Now, consider the transport law for the magnetic field, $\partial\mathbf{B}/\partial t = \boldsymbol{\nabla} \times (\mathbf{v} \times \mathbf{B})$ [Eq. (19.6)]. To linear order, the fluid velocity is $\mathbf{v} = \partial\boldsymbol{\xi}/\partial t$. Inserting this into the transport law, and setting the full magnetic field at fixed $\mathbf{x}$, t equal to the equilibrium field plus its Eulerian perturbation $\mathbf{B} \to \mathbf{B} + \delta\mathbf{B}$, we obtain $\partial\delta\mathbf{B}/\partial t = \boldsymbol{\nabla} \times [(\partial\boldsymbol{\xi}/\partial t) \times (\mathbf{B} + \delta\mathbf{B})]$. Linearizing in the perturbation, and integrating in time, we obtain for the Eulerian perturbation of the magnetic field:

$$\delta\mathbf{B} = \boldsymbol{\nabla} \times (\boldsymbol{\xi} \times \mathbf{B})\ . \tag{19.44a}$$

Since the current and the field are related, in general, by the linear equation $\mathbf{j} = \boldsymbol{\nabla} \times \mathbf{B}/\mu_0$, their Eulerian perturbations are related in this same way:

$$\delta\mathbf{j} = \boldsymbol{\nabla} \times \delta\mathbf{B}/\mu_0\ . \tag{19.44b}$$

In the equation of mass conservation, $\partial\rho/\partial t + \boldsymbol{\nabla}\cdot(\rho\mathbf{v}) = 0$, we replace the density by its equilibrium value plus its Eulerian perturbation, $\rho \to \rho + \delta\rho$ and replace $\mathbf{v}$ by $\partial\boldsymbol{\xi}/\partial t$, and we linearize in the perturbation to obtain

$$\delta\rho + \rho\boldsymbol{\nabla}\cdot\boldsymbol{\xi} + \boldsymbol{\xi}\cdot\boldsymbol{\nabla}\rho = 0\ . \tag{19.44c}$$

The Lagrangian density perturbation, obtained from this via Eq. (19.43), is

$$\Delta\rho = -\rho\boldsymbol{\nabla}\cdot\boldsymbol{\xi}\ . \tag{19.44d}$$

We assume that, as it moves, the fluid gets compressed or expanded adiabatically (no Ohmic or viscous heating, or radiative cooling). Then the Lagrangian change of pressure ΔP in each fluid element (moving with the fluid) is related to the Lagrangian change of density by

$$\Delta P = \left(\frac{\partial P}{\partial\rho}\right)_s \Delta\rho = \frac{\gamma P}{\rho}\Delta\rho = -\gamma P\boldsymbol{\nabla}\cdot\boldsymbol{\xi}\ , \tag{19.44e}$$

where γ is the fluid's adiabatic index (ratio of specific heats), which might or might not be independent of position in the equilibrium configuration. Correspondingly, the Eulerian perturbation of the pressure (perturbation at fixed location) is

$$\delta P = \Delta P - (\boldsymbol{\xi}\cdot\boldsymbol{\nabla})P = -\gamma P(\boldsymbol{\nabla}\cdot\boldsymbol{\xi}) - (\boldsymbol{\xi}\cdot\boldsymbol{\nabla})P\ . \tag{19.44f}$$

This is the pressure perturbation that appears in the fluid's equation of motion.

By replacing $\mathbf{v} \to \partial\boldsymbol{\xi}/\partial t$, $P \to P + \delta P$ and $\mathbf{B} \to \mathbf{B} + \delta\mathbf{B}$, and $\mathbf{j} \to \mathbf{j} + \delta\mathbf{j}$ in the fluid's equation of motion (19.10) and neglecting gravity, and by then linearizing in the perturbation, we obtain

$$\boxed{\rho\frac{\partial^2\boldsymbol{\xi}}{\partial t^2} = \mathbf{j}\times\delta\mathbf{B} + \delta\mathbf{j}\times\mathbf{B} - \boldsymbol{\nabla}\delta P \equiv \hat{\mathbf{F}}[\boldsymbol{\xi}]}\ . \tag{19.45}$$

Here $\hat{\mathbf{F}}$ is a real, linear differential operator, whose form one can deduce by substituting expressions (19.44a), (19.44b), (19.44f) for $\delta\mathbf{B}$, $\delta\mathbf{j}$, and δP, and $\boldsymbol{\nabla}\times\mathbf{B}/\mu_0$ for $\mathbf{j}$. By performing those substitutions and carefully rearranging the terms, we eventually convert the operator $\hat{\mathbf{F}}$ into the following form, expressed in slot-naming index notation:

$$\boxed{\hat{F}_i[\boldsymbol{\xi}] = \left\{\left[(\gamma-1)P + \frac{B^2}{2\mu_0}\right]\xi_{k;k} + \frac{B_jB_k}{\mu_0}\xi_{j;k}\right\}_{;i} + \left[\left(P + \frac{B^2}{2\mu_0}\right)\xi_{j;i} + \frac{B_jB_k}{\mu_0}\xi_{i;k} + \frac{B_iB_j}{\mu_0}\xi_{k;k}\right]_{;j}}\ . \tag{19.46}$$

Honestly! Here the semicolons denote gradients (partial derivatives in Cartesian coordinates; connection coefficients are required in curvilinear coordinates).

We write the operator $\hat{F}_i$ in the explicit form (19.46) because of its power for demonstrating that $\hat{F}_i$ is self adjoint (Hermitian, with real variables rather than complex): By introducing the Kronecker-delta components of the metric, $g_{ij} = \delta_{ij}$, we can easily rewrite Eq. (19.46) in the form

$$\hat{F}_i[\xi] = (T_{ijkl}\xi_{k;l})_{;j}\ , \tag{19.47}$$

where T_{ijkl} are the components of a fourth rank tensor that is symmetric under interchange of its first and second pairs of indices, $T_{ijkl} = T_{klij}$.

Now, our magnetic-confinement equilibrium configuration (e.g. Fig. 19.6) will typically consist of a plasma-filled interior region $\mathcal{V}$ surrounded by a vacuum magnetic field (which in turn may be surrounded by a wall). Our MHD equations with force operator $\hat{\mathbf{F}}$ are valid only in the plasma region $\mathcal{V}$, and not in vacuum, where the Maxwell equations with small displacement current prevail. We shall use Eq. (19.47) to prove that $\hat{\mathbf{F}}$ is a self-adjoint operator when integrated over $\mathcal{V}$, with the appropriate boundary conditions at the vacuum interface.

Specifically, we contract a vector field $\boldsymbol{\zeta}$ into $\hat{\mathbf{F}}[\boldsymbol{\xi}]$, integrate over $\mathcal{V}$, and perform two integrations by parts to obtain

$$\begin{aligned}\int_{\mathcal{V}} \boldsymbol{\zeta}\cdot\mathbf{F}[\boldsymbol{\xi}]dV &= \int_{\mathcal{V}} \zeta_i (T_{ijkl}\xi_{k;l})_{;j} dV = -\int_{\mathcal{V}} T_{ijkl}\zeta_{i;j}\xi_{k;l} dV = \int_{\mathcal{V}} \xi_i (T_{ijkl}\zeta_{k;l})_{;j} dV \\ &= \int_{\mathcal{V}} \boldsymbol{\xi}\cdot\mathbf{F}[\boldsymbol{\zeta}]dV \ . \end{aligned} \tag{19.48}$$

Here we have discarded the integrals of two divergences, which by Gauss's theorem can be expressed as surface integrals at the fluid-vacuum interface $\partial\mathcal{V}$. Those unwanted surface integrals vanish if $\boldsymbol{\xi}$ and $\boldsymbol{\zeta}$ satisfy

$$T_{ijkl}\xi_{k;l}\zeta_i n_j = 0 \ , \quad \text{and} \quad T_{ijkl}\zeta_{k;l}\xi_i n_j = 0 \ , \tag{19.49}$$

with n_j the normal to the interface ∂V.

Now, $\boldsymbol{\xi}$ and $\boldsymbol{\zeta}$ are physical displacements of the MHD fluid, and as such, they must satisfy the appropriate boundary conditions at the boundary $\partial\mathcal{V}$ of the plasma region $\mathcal{V}$. In the simplest, idealized case, the conducting fluid would extend far beyond the region where the disturbances have appreciable amplitude, so $\boldsymbol{\xi} = \boldsymbol{\zeta} = 0$ at the distant boundary, and Eqs. (19.49) are satisfied. More reasonably, the fluid might butt up against rigid walls at $\partial\mathcal{V}$, where the normal components of $\boldsymbol{\xi}$ and $\boldsymbol{\zeta}$ vanish, guaranteeing again that (19.49) are satisfied. This is fine for liquid mercury or sodium, but not for a hot plasma, which would quickly destroy the walls. For confinement by a surrounding vacuum magnetic field, no current flows outside $\mathcal{V}$ and the displacement current is negligible, so $\boldsymbol{\nabla}\times\delta\mathbf{B} = 0$ there. By combining this with the rest of Maxwell's equations and paying careful attention to the motion of the interface and boundary conditions (19.20) there, one can show, once again, that Eqs. (19.49) are satisfied; see, e.g., Sec. 6.6.2 of Goedbloed and Poedts (2004). Therefore, in all these cases Eq. (19.48) is also true, *which demonstrates the self adjointness (Hermiticity) of* $\hat{\mathbf{F}}$.[1] We shall use this below.

Returning to our perturbed MHD system, we seek its normal modes by assuming a harmonic time dependence, $\boldsymbol{\xi} \propto e^{-i\omega t}$. The first-order equation of motion then becomes

$$\boxed{\hat{\mathbf{F}}[\boldsymbol{\xi}] + \rho\omega^2\boldsymbol{\xi} = 0} \ . \tag{19.50}$$

[1]Self-adjointness can also be deduced from energy conservation without getting entangled in detailed boundary conditions; see, e.g., Sec. 10.4.2 of Bellan (2006).

This is an eigenequation for the fluid's Lagrangian displacement $\boldsymbol{\xi}$, with eigenvalue ω^2. It must be augmented by the boundary conditions (19.20) at the edge $\partial\mathcal{V}$ of the fluid.

By virtue of the elegant, self-adjoint mathematical form (19.47) of the differential operator $\hat{\mathbf{F}}$, our eigenequation (19.50) is of a very special and powerful type, called *Sturm-Liouville*; see any good text on mathematical physics, e.g., Arfken, Weber and Harris (2013), Hassani (2013), or Mathews and Walker (1970). From the general (rather simple) theory of Sturm-Liouville equations, we can infer that all the eigenvalues ω^2 are real, so the normal modes are purely oscillatory ($\omega^2 > 0$, $\boldsymbol{\xi} \propto e^{\pm i|\omega|t}$) or are purely exponentially growing or decaying ($\omega^2 < 0$, $\boldsymbol{\xi} \propto e^{\pm|\omega|t}$). Exponentially growing modes represent instability. Sturm-Liouville theory also implies that all eigenfunctions [labeled by indices "(n)"] with different eigenfrequencies are orthogonal to each other, in the sense that $\int_{\mathcal{V}} \rho \boldsymbol{\xi}^{(n)} \cdot \boldsymbol{\xi}^{(m)} dV = 0$.

****

EXERCISES

Exercise 19.11 *Derivation: Properties of Eigenmodes*
Derive the properties of the eigenvalues and eigenfunctions for perturbations of an MHD equilibrium that are asserted in the next to the last paragraph of Sec. 19.5.1, namely:

(a) For each normal mode the eigenfrequency ω_n is either real or imaginary.

(b) Eigenfunctions $\boldsymbol{\xi}^{(m)}$ and $\boldsymbol{\xi}^{(n)}$ that have different eigenvalues $\omega_m \neq \omega_n$ are orthogonal to each other, $\int \rho \boldsymbol{\xi}^{(m)} \cdot \boldsymbol{\xi}^{(m)} dV = 0$.

****

19.5.2 Z-Pinch: Sausage and Kink Instabilities

We illustrate MHD stability theory using a simple, analytically tractable example: a variant of the Z-pinch configuration of Fig. 19.6a. We consider a long, cylindrical column of a conducting, incompressible liquid such as mercury, with column radius R and fluid density ρ. The column carries a current I longitudinally along its surface (rather than in its interior as in Fig. 19.6a), so $\mathbf{j} = (I/2\pi R)\delta(\varpi - R)\mathbf{e}_z$, and the liquid is confined by the resulting external toroidal magnetic field $B_\phi \equiv B$. The interior of the plasma is field free and at constant pressure P_0. From $\boldsymbol{\nabla} \times \mathbf{B} = \mu_0 \mathbf{j}$, we deduce that the exterior magnetic field is

$$B_\phi \equiv B = \frac{\mu_0 I}{2\pi\varpi} \quad \text{at} \quad \varpi \geq R\,. \tag{19.51}$$

Here (ϖ, ϕ, z) are the usual cylindrical coordinates. This is a variant of the Z-pinch because the z-directed current on the column's surface creates the external toroidal field B, which pinches the column until its internal pressure is balanced by the field's pressure,

$$P_0 = \left(\frac{B^2}{2\mu_0}\right)_{\varpi=R}\,. \tag{19.52}$$

It is quicker and more illuminating to analyze the stability of this Z-pinch equilibrium directly instead of by evaluating $\hat{\mathbf{F}}$, and the outcome is the same. (For a treatment based on $\hat{\mathbf{F}}$, see Ex. 19.14 below). Treating only the most elementary case, we consider small, axisymmetric perturbations with an assumed variation $\boldsymbol{\xi} \propto e^{i(kz-\omega t)}\mathbf{f}(\varpi)$ for some function $\mathbf{f}$. As the magnetic field interior to the column vanishes, the equation of motion $\rho d\mathbf{v}/dt = -\boldsymbol{\nabla}(P+\delta P)$ becomes

$$-\omega^2\rho\xi_\varpi = -\delta P' \ , \qquad -\omega^2\rho\xi_z = -ik\delta P \ , \tag{19.53a}$$

where the prime denotes differentiation with respect to radius ϖ. Combining these two equations, we obtain

$$\xi_z' = ik\xi_\varpi \ . \tag{19.53b}$$

Because the fluid is incompressible, it satisfies $\boldsymbol{\nabla}\cdot\boldsymbol{\xi} = 0$; i.e.,

$$\varpi^{-1}(\varpi\xi_\varpi)' + ik\xi_z = 0 \ , \tag{19.53c}$$

which, with Eq. (19.53b), leads to

$$\xi_z'' + \frac{\xi_z'}{\varpi} - k^2\xi_z = 0 \ . \tag{19.53d}$$

The solution of this equation that is regular at $\varpi = 0$ is

$$\xi_z = AI_0(k\varpi) \quad \text{at } \varpi \le R \ , \tag{19.53e}$$

where A is a constant and $I_n(x)$ is the modified Bessel function $I_n(x) = i^{-n}J_n(ix)$. From Eq. (19.53b) and $dI_0(x)/dx = I_1(x)$, we obtain

$$\xi_\varpi = -iAI_1(k\varpi) \ . \tag{19.53f}$$

Next, we consider the region exterior to the fluid column. As this is vacuum, it must be current-free; and as we are dealing with a purely axisymmetric perturbation, the ϖ component of the Maxwell equation $\boldsymbol{\nabla}\times\delta\mathbf{B} = 0$ (with negligible displacement current) reads

$$\frac{\partial\delta B_\phi}{\partial z} = ik\delta B_\phi = 0 \ . \tag{19.53g}$$

The ϕ component of the magnetic perturbation therefore vanishes outside the column.

The interior and exterior solutions must be connected by the law of force balance, i.e. by the boundary condition (19.19f), [or equivalently (19.20a) with the tildes removed], at the plasma's surface. Allowing for the displacement of the surface and retaining only linear terms, this becomes

$$P_0 + \Delta P = P_0 + (\boldsymbol{\xi}\cdot\boldsymbol{\nabla})P_0 + \delta P = \frac{(B+\Delta B_\phi)^2}{2\mu_0} = \frac{B^2}{2\mu_0} + \frac{B}{\mu_0}(\boldsymbol{\xi}\cdot\boldsymbol{\nabla})B + \frac{B\delta B_\phi}{\mu_0} \ , \tag{19.53h}$$

where all quantities are evaluated at $\varpi = R$. Now, the equilibrium force-balance condition gives us that $P_0 = B^2/2\mu_0$ [Eq. (19.52)] and $\boldsymbol{\nabla}P_0 = 0$. In addition, we have shown that $\delta B_\phi = 0$. Therefore Eq. (19.53h) becomes simply

$$\delta P = \frac{BB'}{\mu_0}\xi_\varpi \ . \tag{19.53i}$$

Substituting δP from Eqs. (19.53a) and (19.53e), B from Eq. (19.51), and ξ_ϖ from Eq. (19.53f), we obtain the dispersion relation

$$\begin{aligned}\omega^2 &= \frac{-\mu_0 I^2}{4\pi^2 R^4 \rho}\,\frac{kRI_1(kR)}{I_0(kR)} \\ &\sim \frac{-\mu_0 I^2}{8\pi^2 R^2 \rho}k^2; \qquad \text{for } k \ll R^{-1} \\ &\sim \frac{-\mu_0 I^2}{4\pi^2 R^3 \rho}k; \qquad \text{for } k \gg R^{-1}\ ,\end{aligned} \tag{19.54}$$

where we have used $I_0(x) \sim 1, I_1(x) \sim x/2$ as $x \to 0$ and $I_1(x)/I_0(x) \to 1$ as $x \to \infty$.

Because I_0 and I_1 are positive for all $kR > 0$, for every wave number k this dispersion relation says that ω^2 is negative. Therefore, ω is imaginary, the perturbation grows exponentially with time, and so *the Z-pinch configuration is dynamically unstable.* If we define a characteristic Alfvén speed by $a = B(R)/(\mu_0\rho)^{1/2}$ [Eq. (19.72) below], then we see that the growth time for modes with wavelength comparable to the column diameter is a few Alfvén crossing times, a few times $2R/a$. This is fast!

This is sometimes called a *sausage instability*, because its eigenfunction $\xi_\varpi \propto e^{ikz}$ consists of oscillatory pinches of the column's radius that resemble the pinches between sausages in a link. This sausage instability has a simple physical interpretation (Fig. 19.10a), one that illustrates the power of the concepts of flux freezing and magnetic tension for developing intuition. If we imagine an inward radial motion of the fluid, then the toroidal loops of magnetic field will be carried inward too and will therefore shrink. As the external field is unperturbed, $\delta B_\phi = 0$, we have $B_\phi \propto 1/\varpi$, whence the surface field at the inward perturbation increases, leading to a larger "hoop" stress or, equivalently, a larger $\mathbf{j} \times \mathbf{B}$ Lorentz force, which accelerates the inward perturbation; see Fig. 19.10a.

So far, we have only considered axisymmetric perturbations. We can generalize our analysis by allowing the perturbations to vary as $\boldsymbol{\xi} \propto \exp(im\phi)$. (Our sausage instability corresponds to $m = 0$.) Modes with $m \geq 1$, like $m = 0$, are also generically unstable. The $m = 1$ modes are known as *kink* modes. In this case, there is a bending of the column, and the field strength is intensified along the inner face of the bend and reduced on the outer face, thereby amplifying the instability (Fig. 19.10b). The incorporation of compressibility, as is appropriate for plasma instead of mercury, introduces only algebraic complexity; the conclusions are unchanged. The column is still highly unstable, and it also remains so, if we distribute the longitudinal current throughout the column's interior, thereby adding

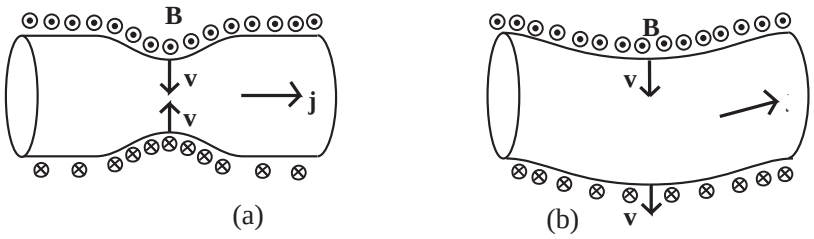

Fig. 19.10: Physical interpretation of a) sausage and b) kink instabilities.

magnetic field to the interior as in Fig. 19.6a.

MHD instabilities such as these have bedevilled attempts to confine plasma for long enough to bring about nuclear fusion. Indeed, considerations of MHD stability were one of the primary motivations for the Tokamak, the most consistently successful of experimental fusion devices.

19.5.3 θ-Pinch and its Toroidal Analog; Flute Instability; Motivation for Tokamak

By contrast with the extreme instability of the Z-pinch configuration, the θ-pinch configuration (Sec. 19.3.3 and Fig. 19.6b) is fully stable against MHD perturbations! (See Ex. 19.12.) This is easily understood physically (Fig. 19.11a). When the plasma cylinder is pinched or bent, at outward displaced regions of the cylinder, the external longitudinal magnetic field lines are pushed closer together, thereby strengthening the magnetic field and its pressure and thence creating an inward restoring force. Similarly, at inward displaced regions, the field lines are pulled apart, weaking their pressure and creating an outward restoring force.

Unfortunately, the θ-pinch configuration cannot confine plasma without closing its ends. The ends can be partially closed by a pair of magnetic mirrors, but there remain losses out the ends that cause problems. The ends can be fully closed by bending the column into a closed torus, but, sadly, the resulting toroidal θ-pinch configuration exhibits a new MHD "flute" instability (Fig. 19.11b).

This flute instability arises on and near the outermost edge of the torus. That edge is curved around the torus's symmetry axis in just the same way as the face of the Z-pinch configuration is curved around its symmetry axis—with the magnetic field in both cases forming closed loops around the axis. As a result, this outer edge is subject to a sausage-type instability, similar to that of the Z-pinch. The resulting corrugations are translated

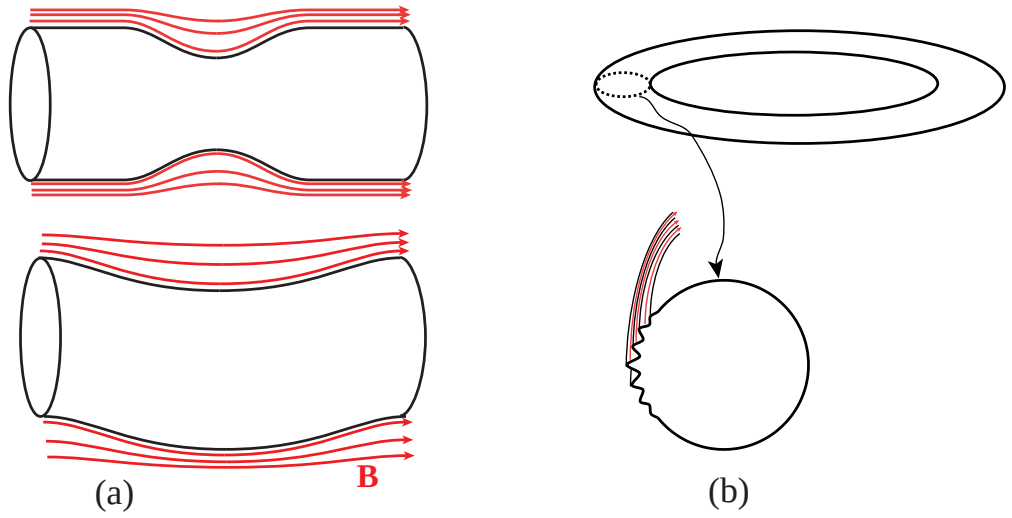

Fig. 19.11: (a) Stabilizing magnetic fields for θ-pinch configuration. (b) Flute intability for θ-pinch configuration made into a torus.

along the torus so they resemble the flutes on a Greek column that supports an architectural arch or roof; hence the name "flute instability". This fluting can also be understood as a flux-tube interchange instability (Ex. 19.13).

The flute instability can be counteracted by endowing the torus with an internal magnetic field that twists (shears) as one goes radially inward (the Tokamak configuration of Fig. 19.6c). Adjacent magnetic surfaces (isobars), with their different field directions, counteract each other's MHD instabilities. The component of the magnetic field along the plasma torus provides a pressure that stabilizes against sausage instabilities and a tension that stabilizes against kink-type instabilities; the component around the torus's guiding circle acts to stabilize its flute modes. In addition, the formation of image currents in the conducting walls of a Tokamak vessel can also have a stabilizing influence.

****

EXERCISES

Exercise 19.12 *Problem: Stability of θ-Pinch*
Derive the dispersion relation $\omega^2(k)$ for axisymmetric perturbations of the θ-pinch configuration, when the magnetic field is confined to the cylinder's exerior, and conclude from it that the θ-pinch is stable against axisymmetric perturbations. [Hint: the analysis of the interior of the cylinder will be the same as for the Z-pinch analyzed in the text.] Repeat your analysis for a general, variable-separated perturbation, of the form $\boldsymbol{\xi} \propto e^{i(m\theta+kz-\omega t)}$ and thereby conclude that the θ-pinch is fully MHD stable.

Exercise 19.13 *Example: Flute Instability Understood by Flux-Tube Interchange*
Carry out an analysis of the flute instability patterned after that for rotating Couette flow (first long paragraph of Sec. 14.6.3) and that for convection in stars (Fig. 18.5): Imagine exchanging two plasma-filled magnetic flux tubes that reside near the outermost edge of the torus. Argue that the one displaced outward will experience an unbalanced outward force, and the one displaced inward will experience an unbalanced inward force. [Some guidance: (i) To simplify the analysis, let the equilibrium magnetic field rise from zero continuously in the outer layers of the torus rather than arising discontinuously at its surface, and consider flux tubes in that outer, continuous region. (ii) Argue that the unbalanced force per unit length on a displaced flux tube is $[-\boldsymbol{\nabla}(P + B^2/2\mu_0) - (B^2_{\rm tube}/\varpi)\mathbf{e}_\varpi]A$. Here A is the tube's cross sectional area, ϖ is distance from the torus's symmetry axis, $\mathbf{e}_\varpi$ is the unit vector pointing away from the symmetry axis, $B_{\rm tube}$ is the field strength inside the displaced tube, and $\boldsymbol{\nabla}(P+B^2/2\mu_0)$ is the net surrounding pressure gradient at the tube's displaced location.] Argue further that the innermost edge of the torus is stable against flux-tube interchange, so the flute instability is confined to the torus's outer face.

****

19.5.4 T2 Energy Principle and Virial Theorems

For the perturbation eigenequation (19.45) and its boundary conditions, analytical or even numerical solutions are only readily obtained in the most simple of geometries and for the

simplest fluids. However, as the eigenequation is self-adjoint, it is possible to write down a variational principle and use it to derive approximate stability criteria. This variational principle has been a powerful tool for analyzing the stability of Tokamak and other magnetostatic configurations.

To derive the variational principle, begin by multiplying the fluid velocity $\dot{\boldsymbol{\xi}} = \partial\boldsymbol{\xi}/\partial t$ into the eigenequation (equation of motion) $\rho\partial^2\boldsymbol{\xi}/\partial t^2 = \hat{\mathbf{F}}[\boldsymbol{\xi}]$. Then integrate over the plasma-filled region $\mathcal{V}$ and use self-adjointness of $\hat{\mathbf{F}}$ to write $\int_{\mathcal{V}} dV\dot{\boldsymbol{\xi}}\cdot\hat{\mathbf{F}}[\boldsymbol{\xi}] = \frac{1}{2}\int_{\mathcal{V}} dV(\dot{\boldsymbol{\xi}}\cdot\hat{\mathbf{F}}[\boldsymbol{\xi}]+\boldsymbol{\xi}\cdot\hat{\mathbf{F}}[\dot{\boldsymbol{\xi}}])$. Thereby obtain

$$\frac{dE}{dt} = 0\ , \quad \text{where} \quad E = T + W\ , \tag{19.55a}$$

$$T = \int_{\mathcal{V}} dV\frac{1}{2}\rho\dot{\boldsymbol{\xi}}^2\ , \quad \text{and} \quad W = W[\boldsymbol{\xi}] \equiv -\frac{1}{2}\int_{\mathcal{V}} dV\boldsymbol{\xi}\cdot\hat{\mathbf{F}}[\boldsymbol{\xi}]\ . \tag{19.55b}$$

The integrals T and W are the perturbation's kinetic and potential energy, and $E = T + W$ is the conserved total energy.

Any solution of the equation of motion $\partial^2\boldsymbol{\xi}/\partial t^2 = \mathbf{F}[\boldsymbol{\xi}]$ can be expanded in terms of a complete set of normal modes $\boldsymbol{\xi}^{(n)}(\mathbf{x})$ with eigenfrequencies ω_n, $\boldsymbol{\xi} = \sum_n A_n\boldsymbol{\xi}^{(n)}e^{-i\omega_n t}$. Because $\hat{\mathbf{F}}$ is a real, self-adjoint operator, these normal modes can all be chosen to be real and orthogonal, even when some of their frequencies are degenerate. As the perturbation evolves, its energy sloshes back and forth between kinetic T and potential W, so time averages of T and W are equal, $\overline{T} = \overline{W}$. This implies, for each normal mode, that

$$\boxed{\omega_n^2 = \frac{W[\boldsymbol{\xi}^{(n)}]}{\int_V dV\frac{1}{2}\rho\boldsymbol{\xi}^{(n)2}}}\ . \tag{19.56}$$

As the denominator is positive definite, we conclude that *a magnetostatic equilibrium is stable against small perturbations if and only if the potential energy $W[\boldsymbol{\xi}]$ is a positive definite functional of the perturbation $\boldsymbol{\xi}$.* This is sometimes called the *Rayleigh Principle* for a general Sturm-Liouville problem. In the MHD context, it is known as the *Energy Principle*.

It is straightforward to verify, by virtue of the self-adjointness of $\hat{\mathbf{F}}[\boldsymbol{\xi}]$, that expression (19.56) serves as an action principle for the eigenfrequencies: If one inserts into (19.56) a trial function $\boldsymbol{\xi}_{\rm trial}$ in place of $\xi^{(n)}$, then the resulting value of (19.56) will be stationary under small variations of $\boldsymbol{\xi}_{\rm trial}$ if and only if $\boldsymbol{\xi}_{\rm trial}$ is equal to some eigenfunction $\boldsymbol{\xi}^{(n)}$; and the stationary value of (19.56) is that eigenfunction's squared eigenfrequency ω_n^2. This action principle is most useful for estimating the lowest few squared frequencies ω_n^2. Because first-order differences between $\boldsymbol{\xi}_{\rm trial}$ and $\boldsymbol{\xi}^{(n)}$ produce second-order errors in ω_n^2, relatively crude trial eigenfunctions can furnish surprisingly accurate eigenvalues.

Whatever may be our chosen trial function $\boldsymbol{\xi}_{\rm trial}$, the computed value of the action (19.56) will always be larger than ω_0^2, the squared eigenfrequency of the most unstable mode. Therefore, if we compute a negative value of (19.56) using some trial eigenfunction, we know that the equilibrium must be even more unstable.

These MHD energy principle and action principle are special cases of the general conservation law and action principle for Sturm-Liouville differential equations; see, e.g., Arfken, Weber and Harris (2013), Hassani (2013), or Mathews and Walker (1970). For further insights into the energy and action principles, see the original MHD paper by Bernstein et. al.

(1958), in which these ideas were developed; also, Chap. 10 of Bellan (2006) and Chap. 6 of Goedbloed and Poedts (2006).

****

EXERCISES

Exercise 19.14 ***T2*** *Example: Reformulation of the Energy Principle; Application to Z-Pinch*

The form (19.46) of the potential energy functional derived in the text is optimal for demonstrating that the operator $\hat{\mathbf{F}}$ is self-adjoint. However, there are several simpler, equivalent forms which are more convenient for practical use.

(a) Use Eq. (19.45) to show that

$$\begin{aligned}\boldsymbol{\xi}\cdot\hat{\mathbf{F}}[\boldsymbol{\xi}] = {}& \mathbf{j}\times\mathbf{b}\cdot\boldsymbol{\xi} - \mathbf{b}^2/\mu_0 - \gamma P(\boldsymbol{\nabla}\cdot\boldsymbol{\xi})^2 - (\boldsymbol{\nabla}\cdot\boldsymbol{\xi})(\boldsymbol{\xi}\cdot\boldsymbol{\nabla})P \\ & + \boldsymbol{\nabla}\cdot[(\boldsymbol{\xi}\times\mathbf{B})\times\mathbf{b}/\mu_0 + \gamma P\boldsymbol{\xi}(\boldsymbol{\nabla}\cdot\boldsymbol{\xi}) + \boldsymbol{\xi}(\boldsymbol{\xi}\cdot\boldsymbol{\nabla})P]\,, \end{aligned} \tag{19.57}$$

where $\mathbf{b}\equiv\delta\mathbf{B}$ is the Eulerian perturbation of the magnetic field.

(b) By inserting Eq. (19.57) into expression (19.55b) for the potential energy $W[\boldsymbol{\xi}]$ and converting the volume integral of the divergence into a surface integral and imposing the boundary condition of vanishing normal component of magnetic field at $\partial\mathcal{V}$ [Eq. (19.20b)], show that

$$\begin{aligned} W[\boldsymbol{\xi}] &= \frac{1}{2}\int_{\mathcal{V}} dV\left[-\mathbf{j}\times\mathbf{b}\cdot\boldsymbol{\xi} + \mathbf{b}^2/\mu_0 + \gamma P(\boldsymbol{\nabla}\cdot\boldsymbol{\xi})^2 + (\boldsymbol{\nabla}\cdot\boldsymbol{\xi})(\boldsymbol{\xi}\cdot\boldsymbol{\nabla})P\right] \\ &\quad -\frac{1}{2}\int_{\partial V} d\boldsymbol{\Sigma}\cdot\boldsymbol{\xi}\left[\gamma P(\boldsymbol{\nabla}\cdot\boldsymbol{\xi}) + \boldsymbol{\xi}\cdot\boldsymbol{\nabla}P - \mathbf{B}\cdot\mathbf{b}/\mu_0\right]\,. \end{aligned} \tag{19.58}$$

(c) Consider axisymmetric perturbations of the cylindrical Z-pinch of an incompressible fluid, as discussed in Sec 19.5.2, and argue that the surface integral vanishes.

(d) Adopt a simple trial eigenfunction and obtain a variational estimate of the growth rate of the sausage instability's fastest growing mode.

Exercise 19.15 ***T2*** *Problem: Potential Energy in Most Physically Interpretable Form*

(a) Show that the potential energy (19.58) can be transformed into the following form

$$\begin{aligned} W[\boldsymbol{\xi}] &= \frac{1}{2}\int_{\mathcal{V}} dV\left[-\mathbf{j}\times\mathbf{b}\cdot\boldsymbol{\xi} + \frac{\mathbf{b}^2}{\mu_0} + \delta P\,\frac{\Delta\rho}{\rho}\right] \\ &\quad +\frac{1}{2}\int_{\partial V} d\boldsymbol{\Sigma}\cdot\boldsymbol{\nabla}\left(\frac{\tilde{B}^2}{2\mu_0} - P - \frac{B^2}{2\mu_0}\right)\xi_n^2 + \frac{1}{2}\int_{\text{vacuum}} dV\,\frac{\tilde{\mathbf{b}}^2}{\mu_0}\,. \end{aligned} \tag{19.59}$$

Here symbols without tildes represent quantities in the plasma region and those with tildes, in the vacuum region; and ξ_n is the component of the fluid displacement orthogonal to the vacuum/plasma interface.

(b) Explain the physical interpretation of each term in this expression for the potential energy. Notice, that, although our original expression for the potential energy, $W = -\frac{1}{2}\int_{\mathcal{V}} \boldsymbol{\xi}\cdot\mathbf{F}[\boldsymbol{\xi}]dV$, entails an integral only over the plasma region, it actually includes the vacuum region's magnetic energy.

Exercise 19.16 ***T2*** *Example: Virial Theorems*

Additional mathematical tools that are useful in analyzing MHD equilibria and their stability, and also useful in astrophysics, are *virial theorems*. In this exercise and the next, we shall deduce time-dependent and time-averaged virial theorems for any system for which the law of momentum conservation can be written in the form

$$\frac{\partial(\rho v_j)}{\partial t} + T_{jk;k} = 0\ . \tag{19.60}$$

Here ρ is mass density, v_j is the material's velocity, ρv_j is momentum density, and T_{jk} is the stress tensor. We have met this formulation of momentum conservation in elastodynamics [Eq. (12.2b)], in fluid mechanics with self gravity [Eq. (2) of Box 13.4], and in magnetohydrodynamics with self gravity [Eq. (19.12)].

The virial theorems involve integrals over any region $\mathcal{V}$ for which there is no mass flux or momentum flux across its boundary: $\rho v_j n_j = T_{jk}n_k = 0$ everywhere on $\partial\mathcal{V}$, where n_j is the normal to the boundary. [Note: if self gravity is included, then the boundary will have to be at spatial infinity (i.e. no boundary), as $T^{\rm grav}_{jk}n_k$ cannot vanish everywhere on a finite enclosing wall.] For simplicity we will use Cartesian coordinates so there are no connection coefficients to worry about, and momentum conservation becomes $\partial(\rho v_j) + \partial T_{jk}/\partial x_k = 0$.

(a) Show that mass conservation $\partial\rho/\partial t + \boldsymbol{\nabla}\cdot(\rho\mathbf{v}) = 0$ implies that for any field f (scalar, vector, or tensor),

$$\frac{dl}{dt}\int_{\mathcal{V}}\rho f dV = \int_{\mathcal{V}}\rho\frac{df}{dt}dV\ , \tag{19.61}$$

(b) Use this relation to show that

$$\boxed{\frac{d^2I_{jk}}{dt^2} = 2\int_{\mathcal{V}} T_{jk}dV}\ , \tag{19.62a}$$

where I_{jk} is the second moment of the mass distribution:

$$I_{jk} = \int_{\mathcal{V}}\rho x_j x_k dV \tag{19.62b}$$

with x_j distance from a chosen origin. This is the *time-dependent tensor virial theorem.*

[Note: the system's mass quadrupole moment is the trace-free part of I_{jk}, $\mathcal{I}_{jk} = I_{jk} - \frac{1}{3}Ig_{jk}$, and the system's moment of inertia tensor is $\mathfrak{I}_{jk} = I_{jk} - Ig_{jk}$, where $I = I_{jj}$ is the trace of I_{jk}.]

(c) If the time integral of d^2I_{jk}/dt^2 vanishes, then the time averaged stress tensor satisfies

$$\boxed{\int_{\mathcal{V}} \bar{T}_{jk} dV = 0} \,. \tag{19.63}$$

This is the *time-averaged tensor virial theorem.* Under what circumstances is this true?

Exercise 19.17 ***T2*** *Example: Scalar Virial Theorems*

(a) By taking the trace of the time-dependent tensorial virial theorem and specializing to an MHD plasma with (or without) self gravity, show that

$$\boxed{\frac{1}{2}\frac{d^2I}{dt^2} = 2E_{\rm kin} + E_{\rm mag} + E_{\rm grav} + 3E_P} \,, \tag{19.64a}$$

where I is the trace of I_{jk}, $E_{\rm kin}$ is the system's kinetic energy, $E_{\rm mag}$ is its magnetic energy, E_P is the volume integral of its pressure, and $E_{\rm grav}$ is its gravitational self energy:

$$\begin{aligned} I &= \int_{\mathcal{V}} \rho \mathbf{x}^2 dV \,, \quad E_{\rm kin} = \int_{\mathcal{V}} \frac{1}{2}\rho \mathbf{v}^2 dV \,, \quad E_{\rm mag} = \int \frac{\mathbf{B}^2}{2\mu_0} \,, \quad E_P = \int_{\mathcal{V}} P dV \,, \\ E_{\rm grav} &= \int_{\mathcal{V}} \rho\Phi = -\int_{\mathcal{V}} \frac{1}{8\pi G}(\boldsymbol{\nabla}\Phi)^2 = -\int_{\mathcal{V}}\int_{\mathcal{V}} \frac{\rho(\mathbf{x})\rho(\mathbf{x}')}{|\mathbf{x}-\mathbf{x}'|} dV' dV \,, \end{aligned} \tag{19.64b}$$

with Φ the gravitational potential energy.

(b) When the time integral of d^2I/dt^2 vanishes, then the time average of the right hand side of Eq. (19.64a) vanishes:

$$\boxed{2\bar{E}_{\rm kin} + \bar{E}_{\rm mag} + \bar{E}_{\rm grav} + 3\bar{E}_P} \,. \tag{19.65}$$

This is the *time-averaged scalar virial theorem.* Give examples of circumstances in which it holds.

Equation(19.65) is a continuum analog of the better known scalar virial theorem, $2\bar{E}_{\rm kin} + \bar{E}_{\rm grav} = 0$, for a system that consists of particles that interact via their self gravity — for example, the solar system; see, e.g., Sec. 3.4 of Goldstein, Poole and Safko (2002).

(c) As a simple but important application of the time-averaged scalar virial theorem, show — neglecting self gravity — that it is impossible for internal currents in a plasma to produce a magnetic field that confines the plasma to a finite volume; external currents, e.g. in solenoids, are necessary.

For applications to the oscillation and stability of self-gravitating systems see, e.g., Sec. 118 of Chandrasekhar (1961).

****

19.6 T2 Dynamos and Reconnection of Magnetic Field Lines

As we have already remarked, the time scale for the earth's magnetic field to decay is estimated to be roughly a million years. This means that some process within the earth must be regenerating the magnetic field. This process is known as a *dynamo*. In general, what happens in a dynamo process is that motion of the fluid stretches the magnetic field lines thereby increasing their magnetic energy density, which compensates the decrease in magnetic energy associated with Ohmic decay. The details of how this happens inside the earth are not well understood. However, some general principles of dynamo action have been formulated, and their application to the sun is somewhat better understood (Exs. 19.18 and 19.19).

19.6.1 T2 Cowling's theorem

It is simple to demonstrate the *impossibility* of dynamo action in any time-independent, axisymmetric flow. Suppose that there were such a dynamo configuration, and the time-independent, poloidal (meridional) field had—for concreteness—the form sketched in Fig. 19.12. Then there must be at least one neutral point marked $\mathcal{P}$ (actually a circle about the symmetry axis), where the poloidal field vanishes. However, the curl of the magnetic field does not vanish at $\mathcal{P}$, so there must be a toroidal current j_ϕ there. Now, in the presence of finite resistivity, there must also be a toroidal electric field at $\mathcal{P}$, since

$$j_\phi = \kappa_e[E_\phi + (\mathbf{v}_P \times \mathbf{B}_P)_\phi] = \kappa_e E_\phi. \tag{19.66}$$

Here $\mathbf{v}_P$ and $\mathbf{B}_P$ are the poloidal components of $\mathbf{v}$ and $\mathbf{B}$. The nonzero E_ϕ in turn implies, via $\boldsymbol{\nabla} \times \mathbf{E} = -\partial\mathbf{B}/\partial t$, that the amount of poloidal magnetic flux threading the circle at $\mathcal{P}$ must change with time, violating our original supposition that the magnetic field distribution is stationary.

We therefore conclude that any time-independent, self-perpetuating dynamo must be more complicated than a purely axisymmetric magnetic field. This is known as *Cowling's theorem*.

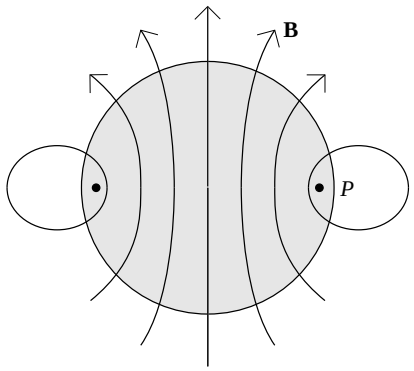

Fig. 19.12: Ä Impossibility of an axisymmetric dynamo.

19.6.2 T2 Kinematic dynamos

The simplest types of dynamo to consider are those in which we specify a particular velocity field and allow the magnetic field to evolve according to the transport law (19.6). Under certain circumstances, this can produce dynamo action. Note that we do not consider, in our discussion, the dynamical effect of the magnetic field on the velocity field.

The simplest type of motion is one in which a *dynamo cycle* occurs. In this cycle, there is one mechanism for creating toroidal magnetic field from poloidal field and a separate mechanism for regenerating the poloidal field. The first mechanism is usually differential rotation. The second is plausibly magnetic buoyancy in which a toroidal magnetized loop is lighter than its surroundings and therefore rises in the gravitational field. As the loop rises, Coriolis forces twist the flow causing poloidal magnetic field to appear. This completes the dynamo cycle.

Small scale, turbulent velocity fields may also be responsible for dynamo action. In this case, it can be shown on general symmetry grounds that the velocity field must contain *helicity*, a non-zero mean value of $\mathbf{v} \cdot \boldsymbol{\omega}$.

If the magnetic field strength grows, then its dynamical effect will eventually react back on the flow and modify the velocity field. A full description of a dynamo must include this back reaction. Dynamos are a prime target for numerical simulations of MHD, and in recent years, significant progress has been made, via simulations, in understanding the terrestrial dynamo and other specialized problems.

****

EXERCISES

Exercise 19.18 ***T2*** *Problem: Differential rotation in the solar dynamo*
This problem shows how differential rotation leads to the production of toroidal magnetic field from poloidal field.

(a) Verify that for a fluid undergoing differential rotation around a symmetry axis with angular velocity $\Omega(r, \theta)$, the ϕ component of the induction equation reads

$$\frac{\partial B_\phi}{\partial t} = \sin\theta \left(B_\theta \frac{\partial \Omega}{\partial \theta} + B_r r \frac{\partial \Omega}{\partial r} \right) , \tag{19.67}$$

where θ is the co-latititude. (The resistive term can be ignored.)

(b) It is observed that the angular velocity on the solar surface is largest at the equator and decreases monotonically towards the poles. There is evidence (though less direct) that $\partial\Omega/\partial r < 0$ in the outer parts of the sun, where the dynamo operates. Suppose that the field of the sun is roughly poloidal. Sketch the appearance of the toroidal field generated by the poloidal field.

Exercise 19.19 ***T2*** *Problem: Buoyancy in the solar dynamo*
Consider a slender flux tube in magnetostatic equilibrium in a conducting fluid. Assume that the diameter of the flux tube is much less than its length, and than its radius of curvature

R, and than the external pressure scale height H; and assume that the magnetic field is directed along the tube, so there is negligible current flowing along the tube.

(a) Show that the requirement of magnetostatic equilibrium implies that

$$\boldsymbol{\nabla}\left(P + \frac{B^2}{2\mu_0}\right) = 0\ . \tag{19.68}$$

(b) Assume that the tube makes a complete circular loop of radius R in the equatorial plane of a spherical star. Also assume that the fluid is isothermal with temperature T, so the pressure scale height is $H = k_B T/\mu g$, where μ is the mean molecular weight and g is the acceleration of gravity. Prove that magnetostatic equilibrium is possible only if $R = 2H$.

(c) In the solar convection zone, $H \ll R/2$. What happens to the toroidal field produced by differential rotation? Suppose the toroidal field breaks through the solar surface. What direction must the field lines have to be consistent with the previous example?

For further insight into the solar dynamo see, e.g. Secs. 8.2 and 8.3 of Goedbloed and Poedts (2004).

****

19.6.3 T2 Magnetic Reconnection

So far, our discussion of the evolution of the magnetic field has centered on the induction equation (19.6) (the magnetic transport law). We have characterized our magnetized fluid by a magnetic Reynolds number using some characteristic length L associated with the flow, and have found that, when $R_M \gg 1$, Ohmic dissipation and field-line diffusion in the transport law are unimportant. This is reminiscent of the procedure we followed when discussing vorticity. However, for vorticity we discovered a very important exception to an uncritical neglect of viscosity, dissipation, and vortex-line diffusion at large Reynolds numbers, namely boundary layers (Sec. 14.4). In particular, we found that large-Reynolds-number flows near solid surfaces will develop very large velocity gradients on account of the no-slip boundary condition, and that the local Reynolds number can thereby decrease to near unity, allowing viscous stress to change the character of the flow completely. Something very similar, called *magnetic reconnection*, can happen in hydromagnetic flows with large R_M, even without the presence of solid surfaces:

Consider two oppositely magnetized regions of conducting fluid moving toward each other (the upper and lower regions in Fig. 19.13). There will be a mutual magnetic attraction of the two regions as magnetic energy would be reduced if the two sets of field lines were superposed. However, strict flux freezing prevents superposition. Something has to give. What happens is a compromise. The attraction causes large magnetic gradients to develop, accompanied by a buildup of large current densities, until Ohmic diffusion ultimately allows

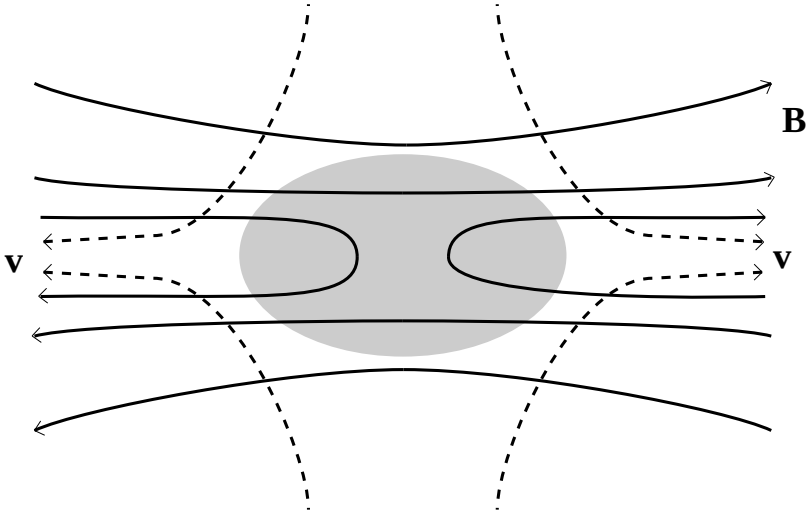

Fig. 19.13: Illustration of magnetic reconnection. In the shaded reconnection region, Ohmic diffusion is important and allows Magnetic field lines to "exchange partners", changing the overall field topology. Magnetic field components perpendicular to the plane of the illustration do not develop large gradients and so do not inhibit the reconnection process.

the magnetic field lines to slip sideways through the fluid and to *reconnect* with field in the other region (the sharply curved field lines in Fig. 19.13).

This reconnection mechanism can be clearly observed at work within Tokamaks and at the earth's magnetopause, where the solar wind's magnetic field meets the earth's magnetosphere. However, the details of the reconnection mechanism are quite complex, involving plasma instabilities and shock fronts. Large, inductive electric fields can also develop when the magnetic geometry undergoes rapid change. This can happen in the reversing magnetic field in the earth's *magnetotail*, leading to the acceleration of charged particles that impact the earth during a *magnetic substorm*.

Like dynamo action, reconnection has a major role in determining how magnetic fields actually behave in both laboratory and space plasmas.

For further detail on the physics and observations of reconnection, see, e.g., Birn and Priest (2007).

19.7 Magnetosonic Waves and the Scattering of Cosmic Rays

In Sec. 19.5, we discussed global perturbations of a non-uniform magnetostatic plasma and described how they may be unstable. We now consider a different, particularly simple example of dynamical perturbations: planar, monochromatic, propagating waves in a uniform, magnetized, conducting medium. These are called *magnetosonic waves*. They can be thought of as sound waves that are driven not just by gas pressure but also by magnetic pressure and tension.

Although magnetosonic waves have been studied experimentally under laboratory con-

ditions, there the magnetic Reynolds numbers are generally quite small so the waves damp quickly via Ohmic dissipation. No such problem arises in space plasmas, where magnetosonic waves are routinely studied by the many spacecraft that monitor the solar wind and its interaction with planetary magnetospheres. It appears that these modes perform an important function in space plasmas; they control the transport of cosmic rays. Let us describe some of the properties of cosmic rays before giving a formal derivation of the magnetosonic-wave dispersion relation.

19.7.1 Cosmic Rays

Cosmic rays are the high-energy particles, primarily protons, that bombard the earth's magnetosphere from outer space. They range in energy from $\sim$ 1MeV to $\sim 3 \times 10^{11}$GeV $= 0.3$ ZeV$\sim$ 50 J. (The highest cosmic-ray energy ever measured was 50 J.) Thus, naturally occurring particle accelerators are far more impressive than their terrestrial counterparts which can only reach to $\sim$ 10 TeV $= 10^4$ GeV!) Most sub-relativistic particles originate within the solar system. Their relativistic counterparts, up to energies $\sim$ 100 TeV, are believed to come mostly from interstellar space, where they are accelerated by expanding shock waves created by supernova explosions (cf. Sec. 17.6.3). The origin of the highest energy particles, above $\sim$ 100 TeV, is an intriguing mystery.

The distribution of cosmic ray arrival directions at earth is inferred to be quite isotropic (to better than one part in 10^4 at an energy of 10 GeV). This is somewhat surprising because their sources, both within and beyond the solar system, are believed to be distributed anisotropically, so the isotropy needs to be explained. Part of the reason for the isotropization is that the interplanetary and interstellar media are magnetized, and the particles gyrate around the magnetic field with the gyro (relativistic cyclotron) frequency $\omega_G = eBc^2/\mathcal{E}$, where $\mathcal{E}$ is the (relativistic) particle energy including rest mass, and B is the magnetic field strength. The gyro (Larmor) radii of the non-relativistic particle orbits are typically small compared with the size of the solar system, and those of the relativistic particles are typically small compared with characteristic length scales in the interstellar medium. Therefore, this gyrational motion can effectively erase any azimuthal asymmetry around the field direction. However, this does not stop the particles from streaming away from their sources along the magnetic field, thereby producing anisotropy at earth. So something else must be impeding this along-line flow, by scattering the particles, causing them to effectively diffuse along and across the field through interplanetary and interstellar space.

As we shall verify in Chap. 20 below, Coulomb collisions are quite ineffective, and if they were effective, then they would cause huge cosmic-ray energy losses in violation of observations. We therefore seek some means of changing a cosmic ray's momentum, without altering its energy significantly. This is reminiscent of the scattering of electrons in metals, where it is phonons (elastic waves in the crystal lattice) that are responsible for much of the scattering. It turns out that in the interstellar medium, magnetosonic waves can play a role analogous to phonons, and scatter the cosmic rays. As an aid to understanding this, we now derive the waves' dispersion relation.

19.7.2 Magnetosonic Dispersion Relation

Our procedure for deriving the dispersion relation (last paragraph of Sec. 7.2.1) should be familiar by now. We consider a uniform, isentropic, magnetized fluid at rest, we perform a linear perturbation, and we seek monochromatic, plane-wave solutions varying $\propto e^{i(\mathbf{k}\cdot\mathbf{x}-\omega t)}$. We ignore gravity and dissipative processes (specifically viscosity, thermal conductivity and electrical resistivity), as well as gradients in the equilibrium, which can all be important in one circumstance or another.

It is convenient to use the velocity perturbation $\delta\mathbf{v}$ as the independent variable. The perturbed and linearized equation of motion (19.10) then takes the form

$$-i\rho\omega\delta\mathbf{v} = -iC^2\mathbf{k}\delta\rho + \delta\mathbf{j}\times\mathbf{B}\ . \tag{19.69}$$

Here C is the sound speed $[C^2 = (\partial P/\partial\rho)_s = \gamma P/\rho]$, not to be confused with the speed of light c, and $\delta P = C^2\delta\rho$ is the Eulerian pressure perturbation for our homogeneous equilibrium. (Note that $\boldsymbol{\nabla}P = \boldsymbol{\nabla}\rho = 0$, so Eulerian and Lagrangian perturbations are the same.) The perturbed equation of mass conservation, $\partial\rho/\partial t + \boldsymbol{\nabla}\cdot(\rho\mathbf{v}) = 0$, becomes

$$\omega\delta\rho = \rho\mathbf{k}\cdot\delta\mathbf{v}\ , \tag{19.70}$$

and Faraday's law $\partial\mathbf{B}/\partial t = -\boldsymbol{\nabla}\times\mathbf{E}$ and the MHD law of magnetic-field transport with dissipation ignored, $\partial\mathbf{B}/\partial t = \boldsymbol{\nabla}\times(\mathbf{v}\times\mathbf{B})$, become

$$\begin{aligned}\omega\delta\mathbf{B} &= \mathbf{k}\times\mathbf{E}\\ &= -\mathbf{k}\times(\delta\mathbf{v}\times\mathbf{B})\ .\end{aligned} \tag{19.71}$$

We introduce the Alfvén velocity

$$\boxed{\mathbf{a} \equiv \frac{\mathbf{B}}{(\mu_0\rho)^{1/2}}}\ , \tag{19.72}$$

and insert $\delta\rho$ [Eq. (19.70)] and $\delta\mathbf{B}$ [Eq. (19.71)] into Eq. (19.69)] to obtain

$$[\mathbf{k}\times\{\mathbf{k}\times(\delta\mathbf{v}\times\mathbf{a})\}]\times\mathbf{a} + C^2(\mathbf{k}\cdot\delta\mathbf{v})\mathbf{k} = \omega^2\delta\mathbf{v}\ . \tag{19.73}$$

This is an eigenequation for the wave's squared frequency ω^2 and eigendirection $\delta\mathbf{v}$. The straightforward way to solve it is to rewrite it in the standard matrix form $M_{ij}\delta v_j = \omega^2\delta v_i$ and then use standard matrix (determinant) methods. It is quicker, however, to seek the three eigendirections $\delta\mathbf{v}$ and eigenfrequencies ω one by one, by projection along preferred directions:

We first seek a solution to Eq. (19.73) for which $\delta\mathbf{v}$ is orthogonal to the plane formed by the unperturbed magnetic field and the wave vector, $\delta\mathbf{v} = \mathbf{a}\times\mathbf{k}$ up to a multiplicative constant. Inserting this $\delta\mathbf{v}$ into Eq. (19.73), we obtain the dispersion relation

$$\boxed{\omega = \pm\mathbf{a}\cdot\mathbf{k}\ ; \qquad \frac{\omega}{k} = \pm a\cos\theta}\ , \tag{19.74}$$

where θ is the angle between $\mathbf{k}$ and the unperturbed field, and $a \equiv |\mathbf{a}| = B/(\mu_o\rho)^{1/2}$ is the Alfvén speed. This type of wave is known as the *Intermediate mode* and also as the *Alfvén*

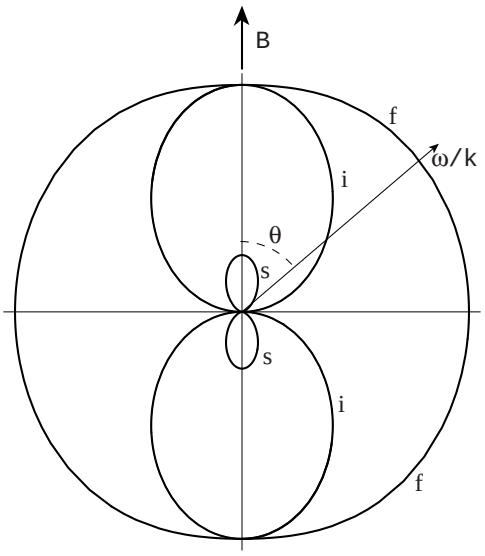

Fig. 19.14: Phase velocity surfaces for the three types of magnetosonic modes, fast (f), intermediate (i) and slow(s). The three curves are polar plots of the wave phase velocity ω/k in units of the Alfvén speed $a = B/\sqrt{\mu_0\rho}$. In the particular example shown, the sound speed C is half the Alfvén speed.

mode. Its phase speed $\omega/k = a\cos\theta$ is plotted as the larger figure-8 curve in Fig. 19.14. The velocity and magnetic perturbations $\delta\mathbf{v}$ and $\delta\mathbf{B}$ are both along the direction $\mathbf{a}\times\mathbf{k}$, so the Alfvén wave is fully transverse; and there is no compression ($\delta\rho = 0$), which accounts for the absence of the sound speed C in the dispersion relation. This Alfvén mode has a simple physical interpretation in the limiting case when $\mathbf{k}$ is parallel to $\mathbf{B}$. We can think of the magnetic field lines as strings with tension B^2/μ_0 and inertia ρ, which are plucked transversely. Their transverse oscillations then propagate with speed $\sqrt{\text{tension/inertia}} = B/\sqrt{\mu_0\rho} = a$. For details and delicacies, see Ex. 21.8.

The dispersion relations for the other two modes can be deduced by projecting the eigenequation (19.73) successively along $\mathbf{k}$ and along $\mathbf{a}$ to obtain the two scalar equations

$$\begin{aligned}(\mathbf{k}\cdot\mathbf{a})(\mathbf{a}\cdot\delta\mathbf{v})k^2 &= \{(a^2+C^2)k^2-\omega^2\}(\mathbf{k}\cdot\delta\mathbf{v})\ ,\\ (\mathbf{k}\cdot\mathbf{a})(\mathbf{k}\cdot\delta\mathbf{v})C^2 &= \omega^2(\mathbf{a}\cdot\delta\mathbf{v})\ .\end{aligned} \tag{19.75}$$

Combining these equations, we obtain the dispersion relation

$$\boxed{\left(\frac{\omega}{k}\right)^2 = \pm\frac{1}{2}(a^2+C^2)\left\{1\pm\left(1-\frac{4C^2a^2\cos^2\theta}{(a^2+C^2)^2}\right)^{1/2}\right\}}\ . \tag{19.76}$$

(By inserting this dispersion relation, with the upper or lower sign, back into Eqs. (19.75), we can deduce the mode's eigendirection $\delta\mathbf{v}$.) This dispersion relation tells us that ω^2 is positive and so there are no unstable modes, which seems reasonable as there is no source of free energy. (The same is true, of course, for the Alfvén mode).

These waves are compressive, with the gas being moved by a combination of gas pressure and magnetic pressure and tension. The modes can be seen to be non-dispersive, which is also

to be expected as we have introduced neither a characteristic timescale nor a characteristic length into the problem.

The mode with the plus signs in Eq. (19.76) is called the *fast magnetosonic mode*; its phase speed is depicted by the outer, quasi-circular curve in Fig. 19.14. A good approximation to its phase speed when $a \gg C$ or $a \ll C$ is $\omega/k \simeq \pm(a^2+C^2)^{1/2}$. When propagating perpendicular to $\mathbf{B}$, the fast mode can be regarded as simply a longitudinal sound wave in which the gas pressure is augmented by the magnetic pressure $B^2/2\mu_0$ (adopting a specific heat ratio γ for the magnetic field of 2 as $B \propto \rho$ and so $P_{\rm mag} \propto \rho^2$ under perpendicular compression).

The mode with the minus signs in Eq. (19.76) is called the *slow magnetosonic mode*. Its phase speed (depicted by the inner figure-8 curve in Fig. 19.14) can be approximated by $\omega/k = \pm aC\cos\theta/(a^2+C^2)^{1/2}$ when $a \gg C$ or $a \ll C$. Note that slow mode, like the intermediate mode, but unlike the fast mode, is incapable of propagating perpendicular to the unperturbed magnetic field; see Fig. 19.14. In the limit of vanishing Alfvén speed or vanishing sound speed, the slow mode ceases to exist for all directions of propagation.

In Part VI, we will discover that MHD is a good approximation to the behavior of plasmas only at frequencies below the "ion cyclotron frequency", which is a rather low frequency. For this reason, magnetosonic modes are usually regarded as low-frequency modes.

19.7.3 Scattering of Cosmic Rays

Now let us return to the issue of cosmic ray propagation, which motivated our investigation of magnetosonic modes. Let us consider 100 GeV particles in the interstellar medium. The electron (and ion, mostly proton) density and magnetic field strength in the solar wind are typically $n \sim 10^4$ m^{-3}, $B \sim 100$ pT. The Alfvén speed is then $a \sim 30$ km s^{-1}, much slower than the speeds of the cosmic rays. In analyzing cosmic-ray propagation, a magnetosonic wave can therefore be treated as essentially a magnetostatic perturbation. A relativistic cosmic ray of energy $\mathcal{E}$ has a gyro (relativistic Larmor) radius of $r_G = \mathcal{E}/eBc$, in this case $\sim 3 \times 10^{12}$m. Cosmic rays will be unaffected by waves with wavelength either much greater than or much less than r_G. However waves, especially Alfvén waves, with wavelength matched to the gyro radius will be able to change the particle's *pitch angle* α (the angle its momentum makes with the mean magnetic field direction). If the Alfvén waves in this wavelength range have rms dimensionless amplitude $\delta B/B \ll 1$, then the particle's pitch angle will change by an amount $\delta\alpha \sim \delta B/B$ every wavelength. Now, if the wave spectrum is broadband, individual waves can be treated as uncorrelated so the particle pitch angle changes stochastically. In other words, the particle diffuses in pitch angle. The effective diffusion coefficient is

$$D_\alpha \sim \left(\frac{\delta B}{B}\right)^2 \omega_B \ , \tag{19.77}$$

where $\omega_G = c/r_G$ is the gyro frequency (relativistic analog of cyclotron frequency). The particle will therefore be scattered by roughly a radian in pitch angle every time it traverses a distance $\ell \sim (B/\delta B)^2 r_G$. This is effectively the particle's collisional mean free path. Associated with this mean free path is a spatial diffusion coefficient

$$D_{\mathbf{x}} \sim \frac{\ell c}{3} \ . \tag{19.78}$$

It is thought that $\delta B/B \sim 10^{-1}$ in the relevant wavelength range in the interstellar medium. An estimate of the collision mean free path is then $\ell(100\text{GeV}) \sim 3 \times 10^{14}$m. Now, the thickness of our galaxy's interstellar disk of gas is roughly $L \sim 3\times10^{18}\text{m}\sim 10^4\ell$. Therefore an estimate of the cosmic ray anisotropy is $\sim \ell/L \sim 10^{-4}$, roughly compatible with the measurements. Although this discussion is an oversimplification, it does demonstrate that the cosmic rays in both the interplanetary medium and the interstellar medium can be scattered and confined by magnetosonic waves. This allows their escape to be impeded without much loss of energy, so that their number density and energy density can be maintained at the level observed at earth.

A good question to ask at this point is "Where do the Alfvén waves come from?". The answer turns out to be that they are almost certainly created by the cosmic rays themselves. In order to proceed further and give a more quantitative description of this interaction, we must go beyond a purely fluid description and explore the motions of individual particles. This is where we shall turn next, in Chap. 20.

Bibliographic Note

For intuitive insight into magnetohydrodynamics, we recommend the ancient film by Shercliff (1968).

For textbook introductions to magnetohydrodynamics, we recommend the relevant chapters of Bellan (2006), Boyd and Sanderson (2003) and Schmidt (1979). For far greater detail, we recommend a textbook that deals solely with magnetohydrodynamics: Goedbloed and Poedts (2003) and its advanced supplement Goedbloed and Poedts (2010). For a very readable treatment from the viewpoint of an engineer, with applications to engineering and metallurgy, see Davison (2001).

For the theory of MHD instabilities and applications to magnetic confinement, see the above references, and also Bateman (1978) and the collection of early papers edited by Jeffrey and Taniuti (1966). For applications to astrophysics and space physics, see Kulsrud (2005), Parks (2003) and Parker (1979).

Bibliography

Arfken, George B., Weber, Hans J., and Harris, Frank E. 2013. *Mathematical Methods for Physicists*, seventh edition, Amsterdam: Elsevier.

Bateman, Glenn. 1978. *MHD Instabilities*, Cambridge Mass.: MIT Press.

Bellan, Paul M. 2006. *Fundamentals of Plasma Physics*, Cambridge: Cambridge University Press.

Birn, Joachim and Priest, eric. 2007. *Reconnection of Magnetic Fields*, Cambridge: Cambridge University Press.

Box 19.2
Important Concepts in Chapter 19

- Fundamental MHD concepts and laws
  - Magnetic field $\mathbf{B}$ as primary electromagnetic variable; $\mathbf{E}$, ρ_e, $\mathbf{j}$ expressible in terms of it, Sec. 19.2.1
  - $\mathbf{B}$, $\mathbf{j}$ frame independent in nonrelativistic MHD; $\mathbf{E}$, ρ_e frame dependent, Sec. 19.2.1
  - Magnetic Reynold's number and magnetic diffusion coefficient, Sec. 19.2.1
  - Evolution law for $\mathbf{B}$: freezing into fluid at high magnetic Reynold's number; diffusion through fluid at lower magnetic Reynold's number, Sec. 19.2.1
  - Magnetic force on fluid expressed in various ways: $\mathbf{j} \times \mathbf{B}$, minus divergence of magnetic stress tensor, curvature force orthogonal to $\mathbf{B}$ minus gradient of magnetic pressure orthogonal to $\mathbf{B}$, Sec. 19.2.2
  - Ohmic dissipation and evolution of entropy, Sec. 19.2.2
  - Boundary conditions at a contact discontinuity and at a shock, Sec. 19.2.3
  - Pressure ratio $\beta \equiv P/(B^2/2\mu_0)$, Sec. 19.3.1
- Interaction of vorticity and magnetic fields: tangled $\mathbf{B}$ lines can create vorticity, vorticity can amplify $\mathbf{B}$, dynamos, Secs. 19.2.4 and 19.6
- Hartmann flow: electromagnetic brake, power generator, flow meter, electromagnetic pump, Sec. 19.4
- Controlled fusion via magnetic confinement; confinement geometries (Z-pinch, θ-pinch, Tokamak) and magnetostatic equilibrium, Sec. 19.3
- Stability of magnetostatic (hydromagnetic) equilibria, Sec. 19.5
  - Lagrangian and Eulerian perturbations, linearized dynamical equation for the fluid displacement $\boldsymbol{\xi}$, self-adjointness, Sturm-Liouville eigenequation, Sec. 19.5.1
  - Energy principle (action principle) for eigenfrequencies, Sec. 19.5.4
  - Sausage and kink instabilities for Z-pinch configuration, Sec. 19.5.2
- Reconnection of magnetic field lines, Sec. 19.6.3
- Magnetosonic waves and dispersion relations, Sec. 19.7.2
  - Alfven mode, fast magnetosonic mode, slow magnetosonic mode, Sec. 19.7.2
  - Scattering of cosmic rays by Alfven waves, Sec. 19.7.3
- Rotating magnetospheres, Ex. 19.9
- Solar wind, Ex. 19.10

Boyd, T. J. M. and Sanderson, J. J. 2003. *The Physics of Plasmas*, Cambridge: Cambridge University Press.

Chandrasekhar, S. 1961. *Hydrodynamic and Hydromagnetic Stability*, Oxford: Oxford University Press.

Davidson, P. A. 2001. *An Introduction to Magnetohydrodynamics*, Cambridge: Cambridge University Press.

Goedbloed, H. & Poedts, S. 2004. *Principles of Magnetohydrodynamics, with Applications to Laboratory and Astrophysical Plasmas*, Cambridge: Cambridge University Press.

Goedbloed, H. & Poedts, S. 2004. *Advanced Magnetohydrodynamics*, Cambridge: Cambridge University Press.

Goldstein, Herbert, Poole, Charles and Safko, John 2002. *Classical Mechanics*, New York: Addison Wesley, third edition.

Hassani, Sadri. 2013. *Mathematical Physics: A Modern Introduction to its Foundations*, second edition, Cham Switzerland: Springer.

Jeffrey, A. and Taniuti, T., eds. 1966. *Magnetohydrodynamic Stability and Thermonuclear Confinement: A Collection of Reprints*, New York: Academic Press.

Keilkhacker, M. and the JET Team. 1998. "Fusion physics progress on JET, *Fusion Engineering and Design*, **46**, 273–290.

Kulsrud, Russell M. 2005. *Plasma Physics for Astrophysics*, Princeton: Princeton University Press.

Mathews, J. & Walker, R.L. 1970. *Mathematical Methods of Physics*, New York: W.A. Benjamin.

Parker, Eugene N. 1979. *Cosmical Magnetic Fields*, Oxford: Clarendon Press.

Parks, George K. 2004. *Physics of Space Plasmas: An Introduction*, Boulder, Colorado: Westview Press.

Schmidt, George. 1979. *Physics of High Temperature Plasmas*, New York: Academic Press.

Shapiro, Stuart L. and Teukolsky, Saul A. 1983. *Black Holes, White Dwarfs, and Neutron Stars*, New York: John Wiley and Sons.

Shercliff, J. A. 1968. *Magnetodydrodynamics*, a movie (National Committee for Fluid Mechanics Films); available at `http://web.mit.edu/fluids/www/Shapiro/ncfmf.html` .